Journal of Medicinal Chemistry

Subscriber access provided by EAST TENNESSEE STATE UNIV

Article

Design, Synthesis, and Pharmacological Evaluation of Novel Multi-substituted Pyridin-3-amine Derivatives as Multi-Targeted Protein Kinase Inhibitors for the Treatment of Non-Small Cell Lung Cancer

Wei Zhu, Hui Chen, Yulan Wang, Jiang Wang, Xia Peng, Xian-Jie Chen, Yinglei Gao, Chunpu Li, Yulong He, Jing Ai, Mei-Yu Geng, Mingyue Zheng, and Hong Liu

J. Med. Chem., **Just Accepted Manuscript** • Publication Date (Web): 22 Jun 2017

Downloaded from http://pubs.acs.org on June 22, 2017

Just Accepted

"Just Accepted" manuscripts have been peer-reviewed and accepted for publication. They are posted online prior to technical editing, formatting for publication and author proofing. The American Chemical Society provides "Just Accepted" as a free service to the research community to expedite the dissemination of scientific material as soon as possible after acceptance. "Just Accepted" manuscripts appear in full in PDF format accompanied by an HTML abstract. "Just Accepted" manuscripts have been fully peer reviewed, but should not be considered the official version of record. They are accessible to all readers and citable by the Digital Object Identifier (DOI®). "Just Accepted" is an optional service offered to authors. Therefore, the "Just Accepted" Web site may not include all articles that will be published in the journal. After a manuscript is technically edited and formatted, it will be removed from the "Just Accepted" Web site and published as an ASAP article. Note that technical editing may introduce minor changes to the manuscript text and/or graphics which could affect content, and all legal disclaimers and ethical guidelines that apply to the journal pertain. ACS cannot be held responsible for errors or consequences arising from the use of information contained in these "Just Accepted" manuscripts.

ACS Publications

Journal of Medicinal Chemistry is published by the American Chemical Society. 1155 Sixteenth Street N.W., Washington, DC 20036

Published by American Chemical Society. Copyright © American Chemical Society. However, no copyright claim is made to original U.S. Government works, or works produced by employees of any Commonwealth realm Crown government in the course of their duties.

Design, Synthesis, and Pharmacological Evaluation of Novel Multi-substituted Pyridin-3-amine Derivatives as Multi-Targeted Protein Kinase Inhibitors for the Treatment of Non-Small Cell Lung Cancer

Wei Zhu[†,‡,§,ǀ], Hui Chen[†,§,ǀ], Yulan Wang[†,§,ǀ], Jiang Wang[†,‡,§], Xia Peng[†,§], Xianjie Chen[†,‡,§], Yinglei Gao[†,§], Chunpu Li[†,‡,§], Yulong He[†,‡,§], Jing Ai[*,†,§], Meiyu Geng[†,§], Mingyue Zheng[*,†,§] and Hong Liu[*,†,‡,§]

[†]State Key Laboratory of Drug Research, Shanghai Institute of Materia Medica, Chinese Academy of Sciences, 555 Zu Chong Zhi Road, Shanghai, 201203, China.

[‡]CAS Key Laboratory of Receptor Research, Shanghai Institute of Materia Medica, Chinese Academy of Sciences, 555 Zu Chong Zhi Road, Shanghai 201203, P. R. China.

[§]University of Chinese Academy of Sciences, No.19A Yuquan Road, Beijing 100049, China.

[ǀ] These authors contributed equally to this study.

Abstract:

A novel series of pyridin-3-amine derivatives were designed, synthesized and evaluated as multi-targeted protein kinase inhibitors for the treatment of non-small cell lung cancer (NSCLC). The hit **1** was firstly disclosed by *in silico* screening against fibroblast growth factor receptors (FGFR), which was subsequently validated by *in vitro* experiments. The structure-activity relationship (SAR) of its analogs was then explored to afford novel FGFR inhibitors **2a-2p** and **3a-3q.** Among them, **3m** showed potent inhibition against FGFR1, 2, and 3. Interestingly, compound **3m** not only inhibited various phosphorylation and downstream signaling across different oncogenic forms in FGFR overactivated cancer cells, but also showed nanomolar level inhibition against several other NSCLC-related oncogenes kinases, including RET, EGFR, EGFR/T790M/L858R, DDR2, and ALK. Finally, *in vivo* pharmacology evaluations of **3m** showed significant antitumor activity (TGI = 66.1%) in NCI-H1581 NSCLC xenografts with good PK profiles.

Key words: tyrosine kinase, FGFR inhibitors, virtual screening, antitumor.

Introduction

Lung cancer is one of the most common cancers and non-small cell lung cancer (NSCLC) accounts for 80–85% of all lung cancers.[1] An epidermal growth factor receptor (EGFR) inhibitor has recently been developed and has been shown to be effective against NSCLC as more than 60% of NSCLCs express genetic mutations of EGFR.[2] However, the emergence of drug-resistant variants of NSCLC has greatly reduced the clinical efficacy of EGFR inhibitors such as gefitinib. Multi-targeted tyrosine kinase inhibitors (TKIs), such as sunitinib, motesanib, sorafenib, lapatinib, and vandetanib, have therefore been designed based on these drug-resistant variants. For EGFR-TKIs-resistant patients with unknown driving mechanism, the concept of "cancer driver gene" may help to increase the efficacy of multi-targeted drugs for NSCLC.[3] In recent years, various driver oncogenic genes in NSCLC have been characterized, including EGFR mutation (15-20%), ALK rearrangements (5%), MET amplification, ErbB2 mutations (1-3%), PI3KCA mutation (5-10%), NF1 mutations (5%), KRAS mutations (25-30%), FGFR1 amplifications (15-20%), FGFR 2/3/4 mutations/rearrangements (5-10%), DDR2 mutations (4%), ROS1 rearrangements (1-2%), and RET rearrangements (1-2%), and so on.[4]

FGFRs are highly conserved transmembrane tyrosine kinase receptors. In human, there are four FGFRs that are typical tyrosine kinase receptors (FGFR1-4), and they are involved in several basic biologic processes, including tissue development, angiogenesis, and tissue regeneration.[5,6] An initial screen of 155 squamous cell lung cancer specimens using single nucleotide polymorphism arrays identified focal

amplifications of the FGFR1 gene.[7] Survival of FGFR1-amplified lung cancer cell lines was additionally shown to be dependent on overexpression of the FGFR1 kinase.[8] As shown in Figure 1, there are many FGFR inhibitors in development for NSCLC, including both selective FGFR inhibitors (LY2874455[9]) and multi-targeted TKIs with FGFR activity. Currently, several multi-targeted FGFR inhibitors have been approved for NSCLC treatment, including vandetanib,[10] lenvatinib,[11] nintedanib,[12] ponatinib,[13] and several others are under clinical trial studies (anlotinib,[14] cediranib,[15] lucitanib,[16] brivanib,[17] danusertib,[18] CP-547632,[19] and AT-9283[20]). For example, dovitinib has been investigated as a nonspecific FGFRs inhibitor, and it also targets vascular endothelial growth factor receptor 1/2/3 (VEGFR1/2/3), platelet-derived growth factor receptor α/β (PDGFR-α/β), stem cell factor receptor (c-Kit), FMS-like tyrosine kinase 3 (FLT3), and colony-stimulating factor 1 receptor (CSF1R). In phase II trial, dovitinib exhibited efficacy in patients with advanced squamous NSCLC with FGFR1 amplification.[21] Another example is crizotinib, a dual inhibitor of ALK and ROS1 signaling, showed marked antitumor activity in patients with ROS1 rearranged or ALK-rearranged advanced NSCLC.[22,23] In 2013 and 2016, FDA approved crizotinib for the treatments of patients with advanced NSCLC whose tumors have ROS1 rearrangements or ALK rearrangements, respectively. Since it has now been accepted that NSCLC is not a singular entity but is in fact multiple pathologies with unique molecular signatures, there has been a renewed interest in developing multi-targeted TKIs targeting different signaling pathways and oncogenic drivers for enhancing efficacy and response rates. Discovery

and development of multi-targeted TKIs with FGFR activity is therefore a promising direction for the treatment of NSCLC.

In this study, molecular docking-based virtual screening was used to discover novel FGFR inhibitors, based on the clarification of FGFR kinase structures. Fifty-seven compounds were selected for FGFR1 inhibitor bioactivity testing, and a compound with the pyridin-3-amine scaffold **1** showed high inhibition ratio at a concentration of 50 μM. Further bioactivity testing on compound **1** revealed that this compound possesses a low micromolar level inhibitory activity with IC_{50} value of 3.8 ± 0.5 μM against FGFR1. To improve the inhibition potency of compound **1** against FGFR1, we analyzed its binding mode with FGFR1 and performed a structure-based structural optimization. The most potent compound **3m** displayed nanomolar IC_{50} against FGFR and FGFR-depended cancer cell line. To better understand the pharmacological profile of **3m**, a kinase panel screening on **3m** was performed, the effects of **3m** on protein kinase phosphorylation and downstream signaling were studied, and the antiproliferative effects of **3m** against several cancer cell lines that harboring the oncogenic kinases targeted by **3m** were detected. It was shown that compound **3m** targets several NSCLC related oncogenes kinases with nanomolar $IC_{50,}$ including against FGFRs, RET, EGFR, EGFR/T790M/L858R, DDR2, and ALK. Meanwhile, compound **3m** could inhibit cancer cell lines proliferation harboring frequently occurring oncogenic forms of FGFRs, DDR2, EGFR, and RET. Finally, *in vivo* studies shown that compound **3m** has good pharmacokinetic profiles and *in vivo* activities against NCI-H1581 xenografts for the treatment of NSCLC.

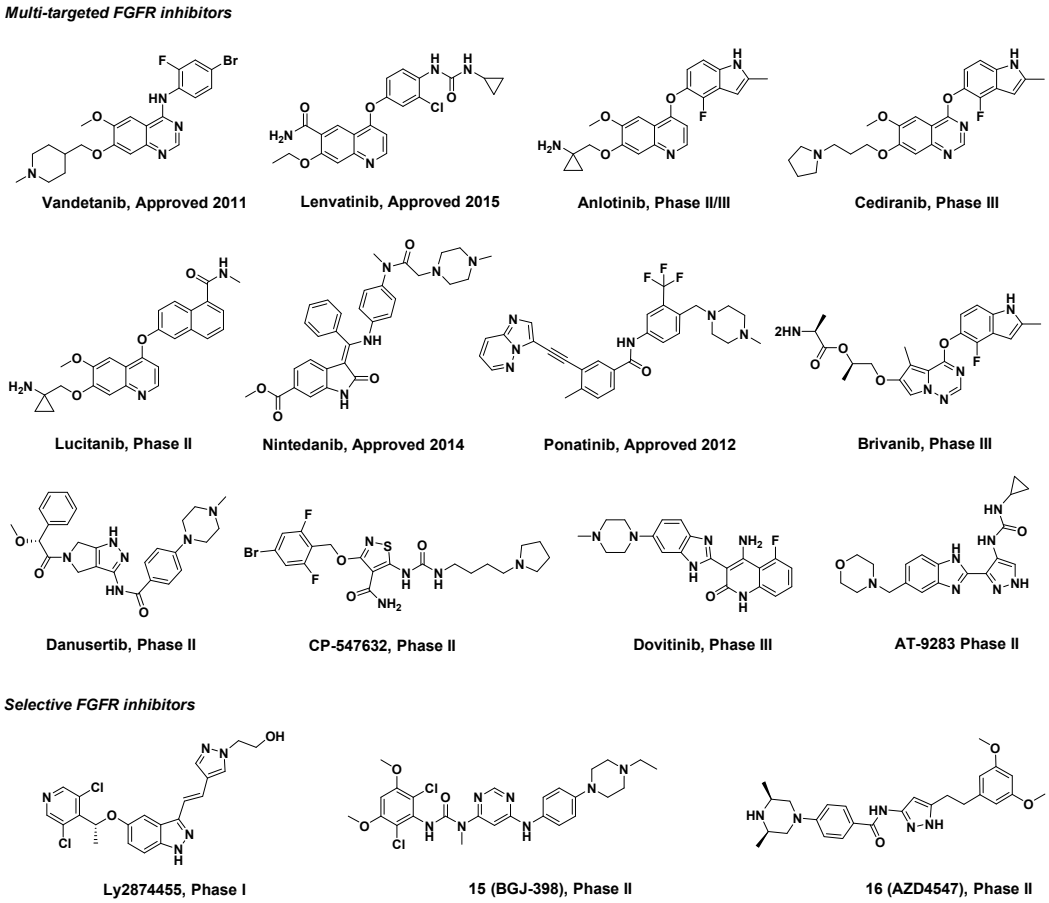

Figure 1. The representative structures of multi-targeted and selective inhibitors with FGFR inhibitory activities for the treatment of NSCLC.

Result and Discussions

Identification and Validation of Multi-substituted Pyridin-3-amine Scaffold by Structure-based Virtual Screening

To discover novel chemotypes of FGFR inhibitors, a docking-based virtual screening[24] was performed on an in-house compound library that contains more than 6,000 compounds with structural diversity.[25-33] The crystal structure of FGFR1 in complex with potency inhibitor **15** (PDB code 3TT0)[34] was used as the receptor for docking by the Schrödinger Suite 2015 software package. The ligand database was prepared with LigPrep module to generate energy minimized three-dimensional (3D) coordinates, in which the protonation states of molecules were calculated with Epik. The crystal structure of receptor was converted into all-atom and refined with the Protein Preparation Wizard in Schrödinger, where the force field used was OPLS3. Finally, the prepared ligands database was docked into prepared receptor with extra precision (XP) mode in Glide module.[35] The top-ranked 1,120 compounds with XP scores lower than -7.0 kcal/mol were kept and the duplicated compounds were removed. Then, the resulting compounds were clustered based on structure similarity using Pipeline Pilot 7.5 software. For each cluster, only one or two compounds with higher docking scores were retained. In the end, by considering both the Glide XP scores and structural diversity, 57 compounds were selected for FGFR1 inhibition assays to validate them in vitro activity. With the ELISA kinase assay at 50 μM, compound **1** showed inhibitory potency with inhibition ratio of 76.5% (Figure 2A).

Further evaluation demonstrated that compound **1** possesses a low micromolar level activity with IC_{50} value of 3.8 ± 0.5 μM against FGFR1.

Binding Mode Analysis of Compound 1

To gain deeper insights into the molecular basis of the inhibitory activity, we analyzed the putative binding mode of compound **1** obtained by molecular docking. As shown in Figure 2B, the active site of FGFR can be generally segmented into three sections: a hinge region, a hydrophobic pocket, and a P-loop region. As depicted in Figure 2B, compound **1** binds in the active site of FGFR1. The pyrazolyl moiety establishes two hydrogen bonds with the backbone amino and carbonyl of Ala564 and Glu562 in the hinge region, and the furyl group is located in the hydrophobic pocket of FGFR protein. The hydroxyl of compound **1** could form a hydrogen bond with the backbone carbonyl of Leu484 in the P-loop, and the amino group may form a weak hydrogen bond with the backbone carbonyl of Glu486. Comparing the putative binding modes of compound **1** with the crystal structures of reported FGFR inhibitors **15** and **16**,[36] we may find that the 3,5-dimethoxy-phenyls of the reported two inhibitors occupy the same hydrophobic pocket of the furyl of compound **1** (Figure 2C). However, the furyl ring doesn't fit the hydrophobic pocket well, which is more spacious and may accommodate a larger group. Intuitively, modifying the furyl group to better fill the hydrophobic pocket is the first round of scheme for the chemical optimization of compound **1**. Cheng *et al.* reported a series of 3,5-disubstutied- pyridine derivatives as CDK inhibitors for the treatment of cancers.[37] Compared with

3,5-disubstutied-pyridine derivatives, the distinct substitutes at the 6-position of the pyridine ring may have great influence on the inhibitory activities against FGFR. Subsequently, the structure−activity relationship (SAR) at P-loop interaction region, hydrophobic pocket, and hinge interaction region of the pyridine core will be further explored (Scheme 1).

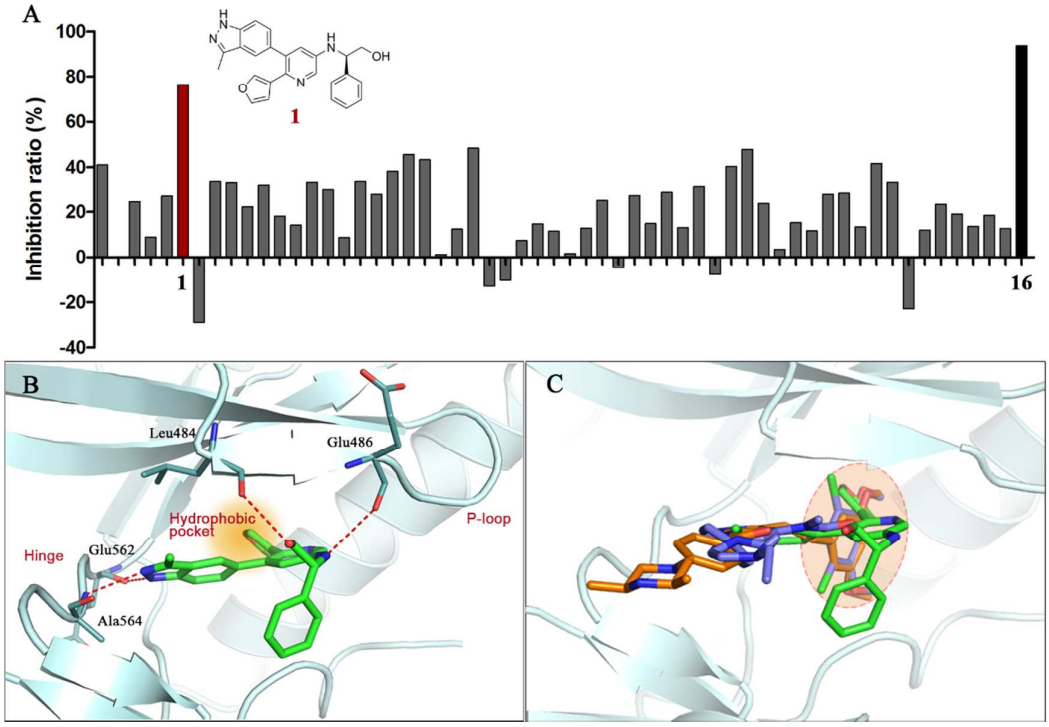

Figure 2. Identification of compound **1** as a hit against FGFR. (A) Inhibitory activity of the 57 selected compounds at 50 μM. Compound **16** (black column) was used as a positive control and the inhibition ratio of compound **1** (red column) is 76.5%. (B) The putative binding mode of compound **1** with FGFR1, where hydrogen bonds are depicted as dashed red lines and hydrophobic pocket of FGFR1 is marked as an orange circle. (C) Superimposition of the binding mode of compound **1** (green) with the crystal structures of compounds **15** (slate) and **16** (orange), where the hydrophobic pocket of FGFR1 is marked as an orange circle.

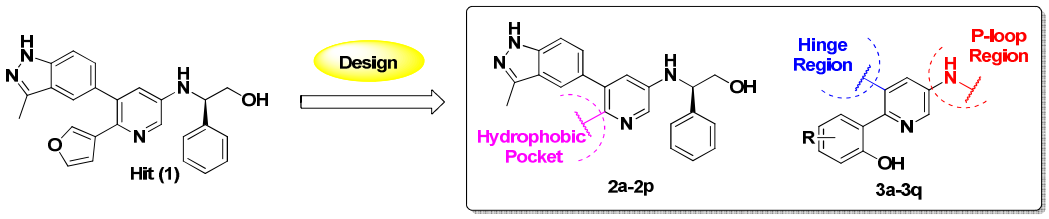

Scheme 1. SAR exploration of pyridin-3-amine derivatives as potent FGFR inhibitors.

Chemistry

Two synthetic routes were exploited to access the desired compounds **2** and **3** (Schemes 2 and 3). With the treatment of Grignard reagent MeMgBr, aldehydes **4** were converted to ethanols, which yielded corresponding ketones **5** upon oxidation of MnO_2 (Scheme 2). Pyrazoles **6** were then prepared by following refluxing with hydrazine hydrate and the following protection with a Boc group. The boronic esters **7** were provided *via* a Miyaura boylation reaction. Pyridin-3-amine **8** underwent Sandmeyer reaction in the presence of NaI, $NaNO_2$, and hydrochloric acid to afford **9**, which was coupled with (*R*)-2-amino-2-phenylethanol with CuI as catalyst to give key intermediate **10**. The Suzuki coupling of **7** and **10** provided chloropyridine **11**, which underwent another coupling with commercial available boronic acids to yield the desired compounds **1**, **2a-2p**, **3a**, and **3k-3q**. The FGFR inhibitors **3b-3e** could be obtained by the coupling of intermediate **12** with different hetero boronic acids and 5-chloro-2-hydroxyphenylboronic acid. As shown in Scheme 3, 3-bromo-2-chloropyridines **13** were prepared by copper catalyzed coupling of intermediate **9** with amino alcohols. The following two-step Suzuki coupling of **13**

with intermediate **7a** and 2-hydroxyphenylboronic acids afforded the desired compound **3f-3j.**

Scheme 2[a]

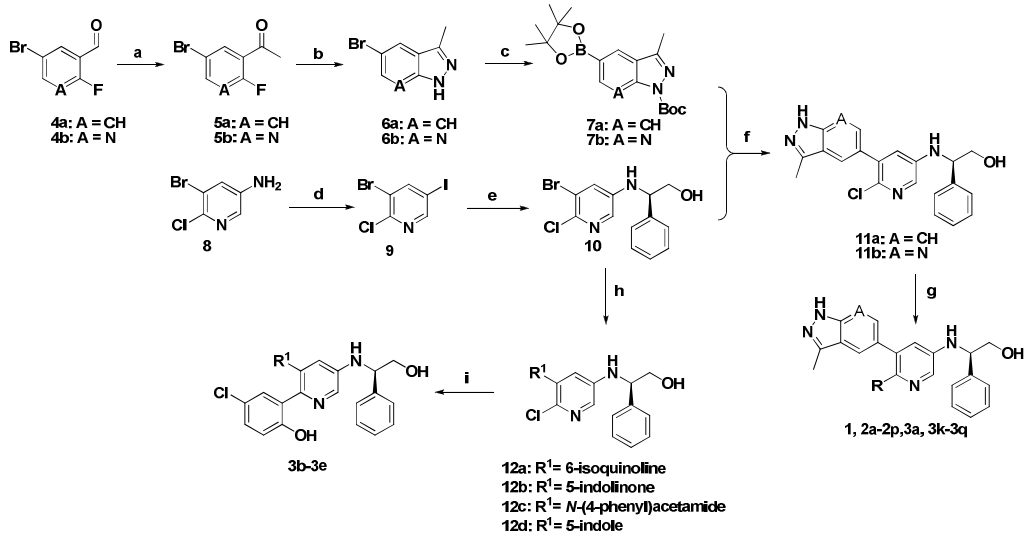

[a] Reagents and conditions: (a) MeMgBr, THF, 0 ^{o}C; then, MnO_2, 1,4-dioxane, reflux; (b) N_2H_4 (75 % in H_2O), reflux; (c) Boc_2O, Et_3N, DCM, r.t.; then, 4,4,4',4‘,5,5,5',5'-octamethyl-2,2'-bi(1,3,2-dioxaborolane), $Pd(dppf)_2Cl_2 \cdot CH_2Cl_2$, KOAc, 1,4-dioxane, 80 ^{o}C; (d) NaI, HCl (6 M), $NaNO_2$, H_2O, 0 ^{o}C – r.t.; (e) (*R*)-2-amino-2-phenyl-ethanol, CuI, K_3PO_4, ethylene glycol, ^{i}PrOH; (f) $Pd(dppf)_2Cl_2 \cdot CH_2Cl_2$, Na_2CO_3, 1,4-dioxane, H_2O, 90 ^{o}C; then TFA, DCM; (g) boronic acids, $Pd(dppf)_2Cl_2 \cdot CH_2Cl_2$, Na_2CO_3, 1,4-dioxane, H_2O, 120 ^{o}C, MW. (h) boronic acids, $Pd(dppf)_2Cl_2 \cdot CH_2Cl_2$, K_2CO_3, 1,4-dioxane, H_2O, 90 ^{o}C; (i) 5-chloro-2-hydroxyphenylboronic acid, $Pd(dppf)_2Cl_2 \cdot CH_2Cl_2$, Na_2CO_3, 1,4-dioxane, H_2O, 120 ^{o}C, MW.

Scheme 3 [a]

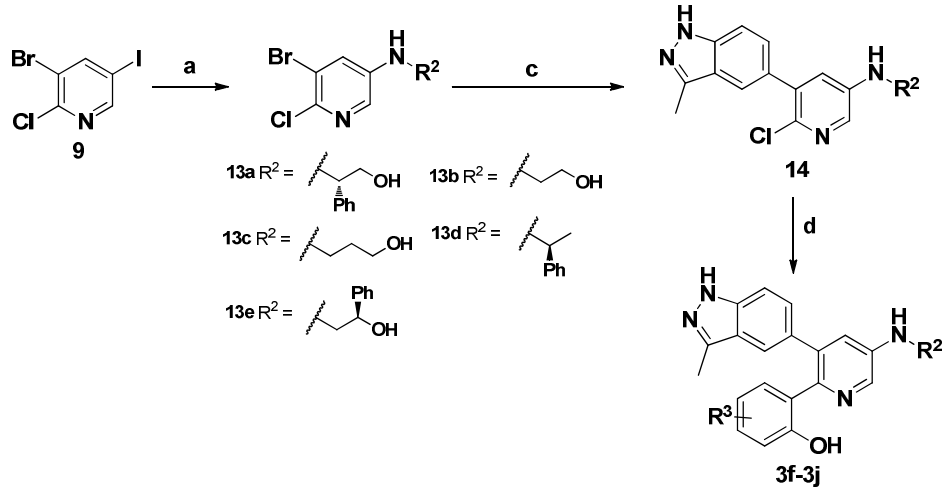

[a] Reagents and conditions: (a) amines, CuI, K_3PO_4, ethylene glycol, ^{i}PrOH; (c) **7a**, $Pd(dppf)_2Cl_2 \cdot CH_2Cl_2$, Na_2CO_3, 1,4-dioxane, H_2O, 90 ^{o}C; then TFA, DCM; (d) boronic acids, $Pd(dppf)_2Cl_2 \cdot CH_2Cl_2$, Na_2CO_3, 1,4-dioxane, H_2O, 120^{o}C, MW.

Structure−Activity Relationships of Multi-Substituted Pyridine-3-amine Derivatives

Based on the modeled complex structure of hit compound **1** with FGFR1, we have designed and synthesized dozens of pyridine-3-amine derivatives to explore their structure and activity (SAR) relationship. As shown in Table 1, the preliminary SAR at the hydrophobic pocket was firstly investigated. Replacement of 3-furan fragment of compound **1** with various heteroaryl moieties or a benzene ring afforded compounds **2a-2g**. Compared with furan and thiophene analogs **2a-2c**, benzene substituted derivative **2d** displayed improved activity. Incorporation of *N*-containing-heteroaryl substituents to yield compounds **2e-2g** resulted in decrease of inhibitory activities. Encouraged by these results, analogs containing substituted

phenyl groups at the 6-position of pyridine nucleus were prepared for further activity optimization (**2h-2p**). Introduction of fluorine (**2h**) had only marginal influence on FGFR inhibition, while trifluoromethyl analog **2i** showed complete loss of activity. Interestingly, compounds **2j-2l**, bearing H-bond donor fragment such as amide or hydroxymethyl group, maintained or slightly enhanced inhibitory activity against FGFR. To our delight, 2-OH substituted derivative **2m** demonstrated potent FGFR inhibition, with an enzymatic IC_{50} of 14.9, 3.0, and 8.0 nM against FGFR1, 2, and 3, respectively. Blocking of the phenolic hydroxyl group (**2n**) led to sharply reduced potency, which indicated the critical role of this potential hydrogen-bond interaction with FGFR. Such pseudo-cyclic motifs have been reported for kinase inhibitor hinge-binders with an intramolecular hydrogen bond. However, based on putative binding mode, it is unlikely to form an internal H-bond in compound **2m** in our case (For details, see Figures S1 and S2 in supporting information). Compared with compound **2m**, 3-OH substituted analog **2o** exhibited 5-fold decreased potency against FGFR1. With the incorporation of chlorine at the 4 position of the phenol moiety in **2m**, compound **2p** also showed potent FGFR inhibition.

Figures 3A and 3B displayed the putative binding modes of compounds **1**, **2d**, and **2p** with FGFR1. Compared with compounds **1** and **2d**, the replacement of furyl to phenyl could gain more hydrophobic shape complementarity with the hydrophobic pocket of FGFR, which is consistent with their inhibitory potency difference in the enzymatic assays. In addition, the phenyl group of **2p** occupies the hydrophobic pocket like **2d**, and the hydroxyl substituent on the phenyl of **2p** could form two hydrogen bonds with

the backbone amino and side chain carboxyl of Asp641. Accordingly, the inhibitory activity of **2p** was improved as compared with **2d**.

Table 1. SAR at the 6-position of the Pyridine Scaffold[a]

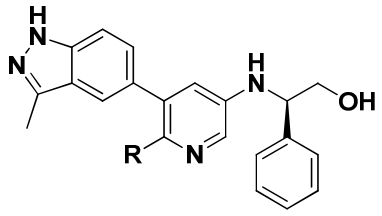

1, **2a-2p**

Compd.	R	FGFR1 (IC_{50}, nM)	FGFR2 (IC_{50}, nM)	FGFR3 (IC_{50}, nM)
1	**furan-3-yl**	3800 ± 500	> 1000	> 1000
2a	**furan-2-yl**	> 1000	100-1000	> 1000
2b	**thiophen-3-yl**	327.4 ± 35.1	56.9 ± 9.0	969.7 ± 236.8
2c	**thiophen-2-yl**	> 1000	100-1000	> 1000
2d	**Ph-**	127.9 ± 13.3	26.3 ± 6.2	279.9 ± 30.5
2e	**pyridin-3-yl**	> 1000	> 1000	> 1000
2f	**quinolin-8-yl**	> 1000	> 1000	> 1000
2g	**indol-7-yl**	456.0 ± 122.4	56.4 ± 5.2	560.7 ± 35.1
2h	**2-F-Ph-**	437.3 ± 113.3	44.6 ± 12.9	430.5 ± 68.1
2i	**2-CF_3-Ph-**	> 1000	> 1000	> 1000
2j	**2-NHAc-Ph-**	418.4 ± 64.6	250.2 ± 49.1	3653.5 ± 283.9
2k	**2-CH_2OH-Ph-**	167.3 ± 49.7	50.5 ± 0.6	250.5 ± 35.6
2l	**2-$CONH_2$-Ph-**	48.8 ± 10.5	72.9 ± 10.3	388.0 ± 73.8
2m	**2-OH-Ph-**	14.9 ± 2.9	3.0 ± 1.0	8.0 ± 1.6
2n	**2-OMe-Ph-**	> 1000	100-1000	> 1000

2o	**3-OH-Ph-**	66.5 ± 5.2	21.4 ± 4.0	433.8 ± 32.3
2p	**2-OH, 5-Cl-Ph-**	55.8 ± 3.9	8.6 ± 2.0	73.1 ± 4.3
16		0.7 ± 0.2	1.1 ± 0.1	5.5 ± 0.4

[a] The IC_{50} values are shown as the mean ± SD (nM) from two separate experiments.

As shown in Table 2, the SARs at the moiety interacting with the hinge region were also explored, with the privileged 4-chloro-phenol fragment retained. As mentioned above, the pyrazole group forms two hydrogen bonds with the hinge region. To investigate the importance of the interaction, we synthesized derivatives **3a**-**3e**, of which the pyrazole group was replaced with other aza-heterocyclic or noncyclic groups (Table 2). Among these derivatives, compound **3a**, isoquinoline analog **3b**, and indolone analog **3c** exhibited similar or slightly increased potency compared with compound **2p**, whereas the ring-opening derivative (**3d**) and indole derivative (**3e**) displayed significantly reduced activity, demonstrating the pivotal role of the hydrogen bond donating group at the hinge region of FGFR. To account for the chemical basis of this result, we analyzed the putative binding modes of **3b** and **3c**. As shown in Figure 3C, **3b** could form one hydrogen bond with the hinge region through quinolyl nitrogen atom to Ala564, and the hydroxyl forms a hydrogen bond with Glu484. Compound **3c** could maintain two hydrogen bonds with the hinge region, while the hydroxyl doesn't form any hydrogen bond interaction, which should be responsible for the decreased inhibitory potency of **3c**. In addition, the noncyclic derivative **3d** and indole-substituted derivative **3e** cannot form stable anchoring

interaction with hinge region, which may lead to its reduced inhibitory activity.

The SAR of the 1-hydroxymethyl-1-phenyl-methylamnio moiety of **2p** was also explored, which interacts with P-loop through two hydrogen bonds based on the model. Either altering the chirality (**3f**) or removing the terminal hydroxyl group (**3g**) resulted in significant loss of potency, highlighting the importance of P-loop region interaction. As shown in Figure 3D, (*R*)-isomer **2p** could form two hydrogen bonds with Leu484 and Glu486 in the P-loop based on the docking, while (*S*)-isomer **3f** only could form one hydrogen bond through the amino to Glu486, thus showing a decreased activity.

Finally, further modification at the phenol segment at the 6-position of the pyridine nucleus led to the preparation of compounds **3k-3q**. The replacement of the chlorine substituent with methyl group (**3k**) retained the potent inhibition against FGFR, however, the bulky isopropyl group (**3l**) led to loss of inhibitory activity. Interestingly, the following F-scan at the phenol moiety afforded a handful of FGFR inhibitors **3m-3q** with significantly enhanced activities, which can be attributed to the feature of relatively small and electron-withdrawing fluorine atom (For details, see **Figure S3** in supporting information). [38,39]

Table 2. SAR of Substituents R^1, R^2 and R^3 on the 2-(Pyridin-2-yl)Phenol Scaffold[a]

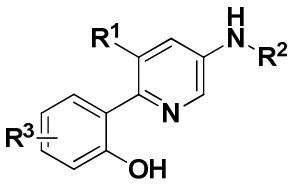

3a-3q

Compd.	R^1	R^2	R^3	FGFR1 (IC_{50}, nM)	FGFR2 (IC_{50}, nM)	FGFR3 (IC_{50}, nM)
3a	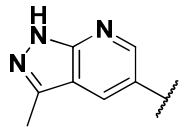	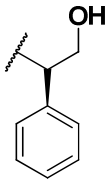	**5-Cl**	24.9 ± 3.1	6.6 ± 1.5	93.9 ± 25.7
3b	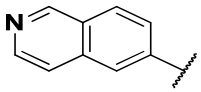	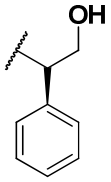	**5-Cl**	16.1 ± 4.5	2.0 ± 0.1	23.0 ± 8.2
3c	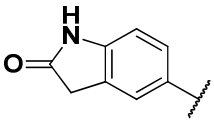	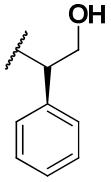	**5-Cl**	91.5 ± 8.5	153.5 ± 11.9	591.5 ± 57.2
3d	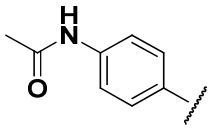	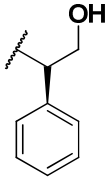	**5-Cl**	>1000	>1000	>1000
3e	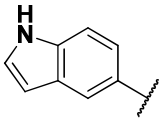	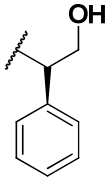	**5-Cl**	>1000	>1000	>1000
3f	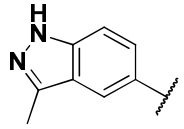	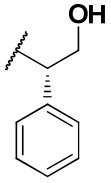	**5-Cl**	>1000	>1000	>1000

3g	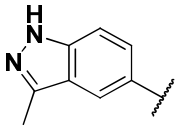	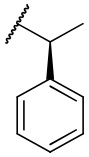	**5-Cl**	>1000	>1000	>1000
3h	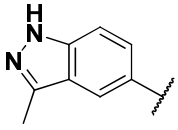	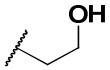	**5-F**	>1000	>1000	>1000
3i	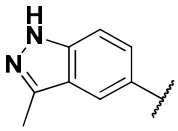	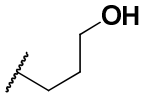	**5-F**	>1000	>1000	>1000
3j	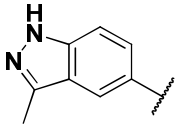	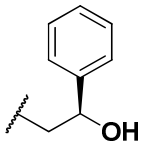	**5-Cl**	168.3 ± 51.7	71.9 ± 26.7	401.5 ± 1.1
3k	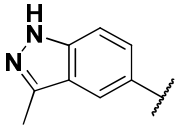	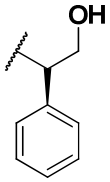	**5-Me**	32.3 ± 10.8	16.1 ± 6.0	22.8 ± 4.9
3l	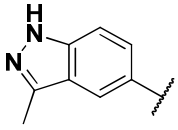	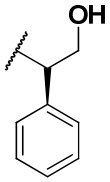	**5-^{i}Pr**	>1000	>1000	>1000
3m	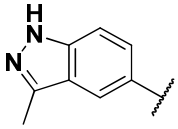	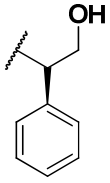	**5-F**	18.0 ± 4.9	1.6 ± 0.3	27.5 ± 9.4
3n	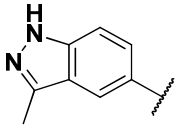	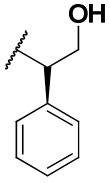	**4-F**	25.2 ± 8.1	4.7 ± 0.7	15.9 ± 0.9
3o	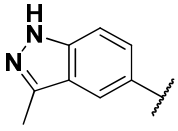	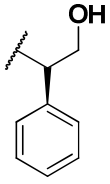	**3-F**	27.9 ± 0.4	2.5 ± 0.8	35.3 ± 4.1

3p	**4,5-di-F**	10.6 ± 1.1	2.8 ± 0.8	27.6 ± 1.1
3q	**3,5-di-F**	63.5 ± 0.2	3.4 ± 0.3	58.4 ± 14.0
16		0.7 ± 0.2	1.1 ± 0.1	5.5 ± 0.4

[a] The IC_{50} values are shown as the mean ± SD (nM) from two separate experiments.

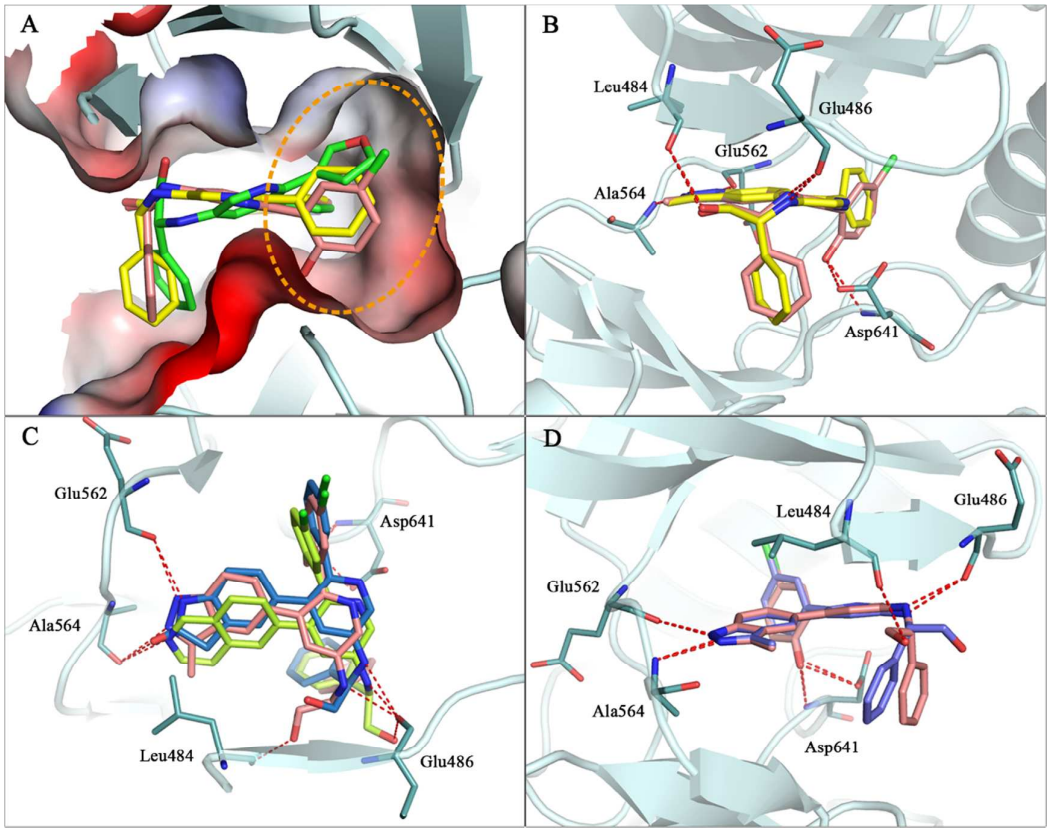

Figure 3. The putative binding modes of pyridine-3-amine derivatives by docking in FGFR1 protein (PDB code: 3TT0). (A) The binding modes of **1** (green), **2d** (yellow) and **2p** (pink) in the hydrophobic pocket of FGFR1, of which the front side of pocket

surface is clipped away for clarity and the hydrophobic pocket is depicted as a dashed orange circle. (B) The binding modes of **2d** (yellow) and **2p** (pink) with FGFR1. (C) Superimposition of the binding modes of **2p** (pink), **3c** (blue), and **3b** (limon). (D) The binding modes of **2p** ((*R*)-isomer) and its enantiomer **3f** ((*S*)-isomer). Hydrogen bonds are depicted as dashed red lines.

Cancer Cell Inhibitory Activities of the Selected Compounds:

Based on the enzymatic inhibitory potency against FGFR, compounds **2d**, **2m**, **2n**, **2p**, **3a**, **3b**, and **3m-3q** were selected to further evaluate their inhibitory activities against FGFR2 amplification cell line SNU16 (Table 3). The pan-FGFR inhibitor **16** was tested as positive control. As shown in Table 3, the selected compounds exhibited moderate to potent inhibition. Overall, the cell-based anti-proliferative results of the selected compounds generally agree with the FGFR inhibition results at the molecular level. Among them, compound **3m** demonstrated best inhibitory activity against cell assay SNU16 with IC_{50} of 24.8 nM, which thus was selected for further investigation.

Table 3. Anti-proliferative Activities of Derivatives against FGFR-Expressing Cancer Cell SNU16 [a]

Compd.	SNU16 (IC_{50}, nM)	Compd.	SNU16 (IC_{50}, nM)
2d	677.7 ± 30.5	**3m**	24.8 ± 0.6
2m	57.5 ± 3.7	**3n**	313.3 ± 25.5

2o	36.2 ± 2.9	**3o**	293.5 ± 27.8
2p	24.8 ± 3.3	**3p**	288.6 ± 84.2
3a	2281.3 ± 20.0	**3q**	280.1 ± 43.5
3b	249.0 ± 44.8	**16**	25.4 ± 1.2

[a] The IC_{50} values are shown as the mean ± SD (nM) from two separate experiments.

Compounds 2p, 3b, 3m, and 3n as multi-target kinase inhibitors

Compounds **2p**, **3b**, **3m**, and **3n** were distinguished for their remarkable potency against recombinant human FGFR kinase. Accordingly, we were prompted to investigate whether this potency was specifically against FGFR. As shown in Table 4, compounds **2p**, **3b**, **3m**, and **3n** also strongly inhibited the kinase activity of KDR, VEGFR-1, Ret, EGFR, DDR2, ABL, ErbB4, and c-Src, with IC_{50} value at nanomole or sub-nanomole level. Compounds **2p**, **3b**, **3m**, and **3n** are, therefore, multi-targeted protein kinase inhibitors.

Given the relative high inhibitory potency of compounds **2p**, **3b**, **3m**, and **3n** against FGFR, RET, DDR2, EGFR and VEGFR2, together with the fact that these kinases are important targetable oncogenes in NSCLC and the most verified targets in cancer therapy, we took these kinases as representatives to evaluate the inhibitory effect of **2p**, **3b**, **3m**, and **3n** on protein kinases-associated events. Interestingly, small structural changes may significantly alter the activity profile of the compounds. For example, compound **3b** is much more potent than **3m** on FGFR4 and EGFR inhibition,

while **3m** is more active than **3b** on IR and IGF1R. Such variance in kinase activity profile may provide opportunity for future fine-tuning the efficacy of the compounds, suggesting that these series of compounds are usefully multi-targeted, instead of nonspecific promiscuous kinase inhibitors. While, compounds **2p**, **3b**, **3m**, and **3n** displayed no obvious inhibitory activity against CDK1, CDK4, and CDK6 (IC_{50} > 1000 nM, Table 4), compared with 3,5-disubstituted-pyridine analogs reported by Cheng et al.[25]

Table 4. The kinase panel screening data of compounds 2p, 3b, 3m, and 3n. [a]

Kinase	IC_{50} (nM)			
	2p	**3b**	**3m**	**3n**
FGFR1	10.1 ± 0.2	12.7 ± 2.6	8.7 ± 1.1	24.4 ± 13.8
FGFR2	8.2 ± 1.3	1.0 ± 0.1	2.4 ± 1.3	5.8 ± 0.5
FGFR3	15.9 ± 3.8	6.0 ± 0.3	7.1 ± 1.7	32.9 ± 0.1
FGFR4	61.7 ± 6.4	7.4 ± 3.2	299.4 ± 34.5	93.3 ± 19.3
KDR	3.7 ± 0.2	0.8 ± 0.0	1.7 ± 0.0	2.6 ± 0.1
Ret	0.7 ± 0.1	0.04 ± 0.01	0.2 ± 0.1	0.4 ± 0.0
EGFR	3.1 ± 1.4	4.2 ± 1.9	4.7 ± 0.1	8.1 ± 6.6
EGFR/T790M/L858R	8.6 ± 2.5	1.9 ± 0.8	6.0 ± 5.9	1.3 ± 0.1
DDR2	-	-	0.8 ± 0.0	-
ABL	6.6 ± 1.8	4.3 ± 0.5	2.9 ± 1.8	6.1 ± 2.5
ErbB4	5.3 ± 4.4	5.0 ± 4.9	6.2 ± 3.7	2.4 ± 0.1
c-Src	3.9 ± 1.8	6.4 ± 4.3	5.7 ± 2.8	6.0 ± 3.7

VEGFR-1	>10	>10	1-10	>10
IR	91.6 ± 21.2	431.2 ± 183.2	417.5 ± 112.6	887.6 ± 163.5
IGF1R	>100	>1000	>1000	>1000
PDGFR-α	>100	>100	>100	>100
PDGFR-β	>100	1-10	>10	1-10
Mer	30.9 ± 13.7	4.4 ± 1.8	36.9 ± 20.8	7.1 ± 2.5
ErbB2	1-10	1-10	>10	1-10
ALK	231.1 ± 14.3	93.9 ± 27.7	101.1 ± 29.3	155.5 ± 10.4
LTK	299.5 ± 123.4	45.3 ± 15.3	122.9 ± 52.4	68.5 ± 11.3
ROS1	272.9 ± 101.3	168.5 ± 87.2	>1000	>1000
EPH-A2	>10	>100	>10	>100
c -Kit	>10	>10	>10	>10
Erk2	960.2 ± 87.4	>1000	574.7 ± 120.1	>1000
c-Met	>1000	196.1 ± 43.7	>1000	>1000
AXL	>1000	>1000	>1000	>1000
Tyro3	>1000	>1000	>1000	>1000
CDK1	>1000	>1000	>1000	>1000
CDK4	>1000	>1000	>1000	>1000
CDK6	>1000	>1000	>1000	>1000

[a] The IC_{50} values are shown as the mean ± SD (nM) from two separate experiments.

Compound 3m blocks protein kinase phosphorylation and downstream signaling in cells.

We then investigated the intracellular targeting activity of compound **3m**. Both naturally and genetically kinase expressing cell lines were tested (Figure 4). Firstly, the effects of compound **3m** on the FGFR phosphorylation and downstream signaling was investigated in representative FGFR-addicted cancer cells. Compound **3m** inhibited the phosphorylation of FGFRs and FGFR substrate 2α (FRS2α), the key adaptor protein largely specific to FGFR, in a dose-dependent manner in the tested cell lines. The phosphorylation of PLCγ and ERK, key downstream molecules of FGFR,[40] was also inhibited upon compound **3m** treatment (Figures 4A-4C). Similar results were observed in DDR2, RET, and KDR-driven NCI-H2286, Ba/F3/CCDC6-RET Ba/F3/TEL-KDR cells, respectively (Figures 4D-4F). Together, compound **3m** exhibited an effective inhibition of FGFR, DDR2, RET, and KDR activation and their signaling.

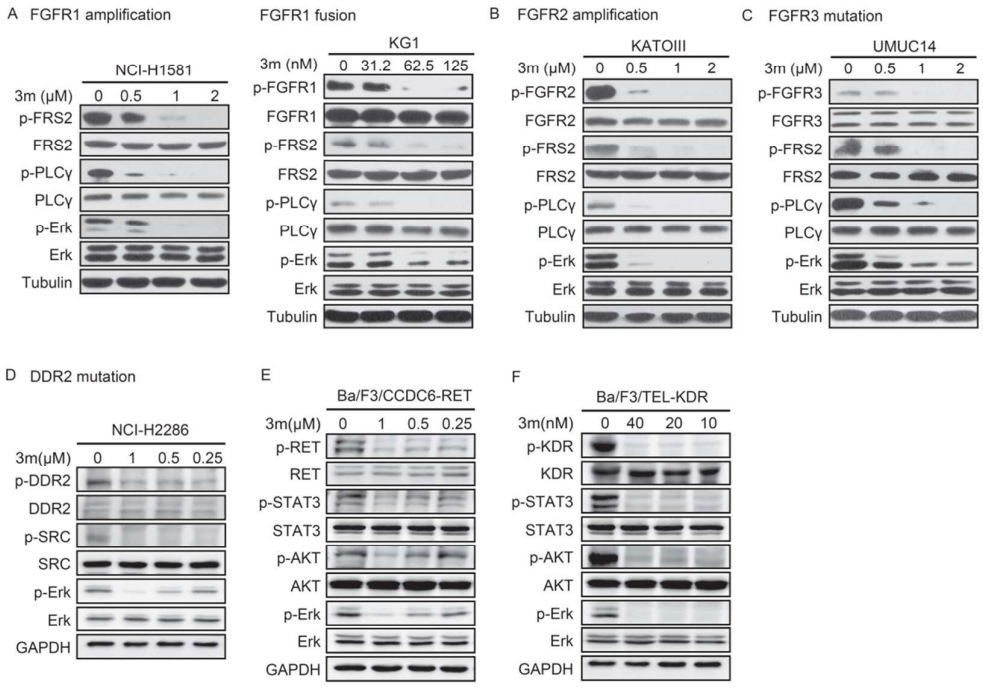

Figure 4. Compound **3m** blocks tyrosine kinase phosphorylation and downstream signaling in cells. Cells including NCI-H1581(A, left), KG1(A, right), KATOIII(B), UMUC14(C), NCI-H2286(D), Ba/F3/CCDC6-RET(E), Ba/F3/TEL-KDR (F) treated with **3m** for 2 h at the indicated concentrations were lysed and subjected to Western blot analysis.

Compound 3m Impairs Cancer Cell Proliferation

To further detect the anti-proliferative effects of compound **3m** targeting the indicated protein kinases, we extended to a panel of human cancer cell and mode cell lines that harboring frequently occurring oncogenic forms of FGFRs, DDR2, EGFR, RET, and KDR (Table 5). As expected, compound **3m** remarkably inhibited cell proliferation of FGFR-addicted cancer cells, including NCI-H1581, KG1, KATOIII, SNU16,

UMUC14, and RT112, with IC_{50} values of 391.2, 14.5, 155.7, 24.8, 128.1, and 122.5 nM, respectively. Moreover, compound **3m** significantly inhibited the proliferation of HCC827 and PC-9 cells, which feature EGFR-dependent cell growth, while compound **3m** inhibited the proliferation of H1975 cells with IC_{50} value of 447.6 nM. Similar observation was also obtained in DDR2, RET, and KDR-constitutively activated NCI-H2286, Ba/F3/CCDC6-RET and Ba/F3/TEL-KDR cells. Our results indicated that **3m** inhibits cancer cell proliferation by targeting multi-kinase.

Table 5. Effects of 3m on cancer cell proliferation. [a]

Cell Line	gene alteration	3m (IC_{50}, nM)	16 (IC_{50}, nM)
NCI-H1581	FGFR1 amplification	391.2 ± 14.5	62.6 ± 5.7
KG1	FGFR1OP2-FGFR1	14.5 ± 4.5	16.1 ± 0.8
KATOIII	FGFR2 amplification	155.7 ± 21.2	14.1 ± 2.5
SNU16	FGFR2 amplification	24.8 ± 0.6	10.5 ± 2.0
UMUC14	FGFR3 mutation	128.1 ± 0.3	27.1 ± 0.1
RT112	FGFR3 amplification	122.5 ± 4.1	27.0 ± 1.8
HCC827	EGFR Exon 19 del	0.4 ± 0.0	/
PC-9	EGFR L858R	5.3 ± 0.4	/
H1975	EGFR T790M/L858R	447.6 ± 45.7	/
NCI-H2286	DDR2 I638F mutation	317.2 ± 22.1	/
Ba/F3/CCDC6-RET	CCDC6-RET fusion	315.7 ± 1.7	/
Ba/F3/TEL-KDR	TEL-KDR fusion	9.8 ± 1.3	/

[a] The IC_{50} values are shown as the mean ± SD (nM) from two separate experiments.

PK Profiles of Compound 3m

Pharmacokinetic (PK) profile of the candidate **3m** was assessed in Sprague−Dawley

(SD) rats and CD-1 mice (Table 6). Compound **3m** proved to be suitable for oral administration with high area under the curve ($AUC_{0-\infty}$ = 18705.5 ng/mL*h), long half-life ($t_{1/2}$ = 8.0 h), and good oral bioavailability (F = 60%) in SD rats. Compound **3m** displayed a lower half-life of 2.72 h and AUC_{0-t} of 2402 ng·h/mL at 20 mg/kg oral administration in CD-1 mice than in SD rats. The binding ratio of plasma protein to **3m** was 99.56%. Accordingly, the free C_{max} for **3m** in the plasma at the dose of 20 mg/kg and 5 mg/kg were calculated as 10.2 and 1.1 nM, respectively.

Table 6. PK profiles of compound 3m in SD rats and CD-1 mice.

Species	Compd.	Dose (mg/kg)	T_{max} h	C_{max} ng/mL	AUC_{0-t} ng/mL*h	$AUC_{0-\infty}$ ng/mL*h	MRT h	$t_{1/2}$ h	CLz L/h/kg	F %
Rats	**3m** (p.o.)	20	1	2077.4	16629.1	18705.5	6.72	8.0	/	60%
	3m (i.v.)	10	0.25	6535.2	13748.4	13756.9	3.41	2.39	0.727	
Mice	**3m** (p.o.)	20	0.42	961	2402	2409	3.59	2.72	/	
	3m (p.o.)	5	1.50	106	289	290	3.74	2.50	/	

In vivo Antitumor Efficacy

Classic FGFR-dependent H1581 lung cancer cell line derived xenograft was used for the *in vivo* efficacy evaluation, nude mice bearing NCI-H1581 tumors were randomized and treated with **3m** at doses of 5 or 20 mg/kg for 14 consecutive days. As shown in Figure 5, compound **3m** could suppress tumor growth in a dose-dependent manner, with the tumor growth inhibition ratio (TGI) of 37.8% and 66.1% at the doses of 5 mg/kg and 20 mg/kg, respectively, indicating compound 3m elicited a marked antitumor efficacy in NCI-H1581 tumor model. However, since adverse reactions such as diarrhea, emaciation and body weight loss were observed in mice dosed at 20 mg/kg, higher dose treatment was not further carried out in this study.

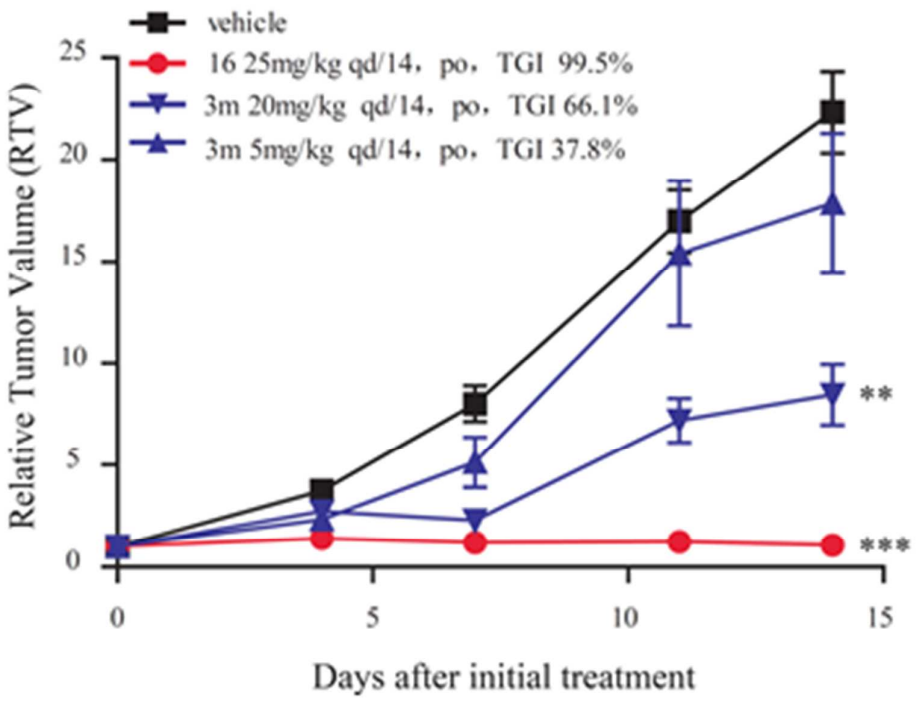

Figure 5. Compound 3m inhibits tumor growth in NCI-H1581 xenografts. The mice were randomly assigned into control vehicle and treatment groups (n = 6 in treated group, n = 12 in vehicle group), when the tumor volume reached 100-150 mm^3. The control groups were given vehicle alone, and the treatment groups received **3m** or 16 at the indicated doses via oral administration once daily for 14 days. The results are expressed as the mean ± SEM. *p<0.05, ** p<0.01,*** p<0.001 *v.s.* control group, determined using Student's t test. The relative tumor volume (RTV) was measured on the final day of the study for the drug-treated mice compared with the control mice.

Conclusion

In summary, a novel series of pyridin-3-amine derivatives were designed, synthesized, and evaluated as multi-targeted protein kinase inhibitors for the treatment of NSCLC.

The hit **1** was disclosed by *in silico* screening and sequential validated by *in vitro* experiments. Based on the binding mode analysis of compound **1** and FGFR kinase domain, SAR focusing on the hydrophobic pocket, hinge region and P-loop region, respectively, was further explored. Among them, compound **3m** showed high potency against FGFR kinase (FGFR1: IC_{50} = 18.0 nM, FGFR2: IC_{50} = 1.6 nM, FGFR3: IC_{50} = 27.5 nM). Furthermore, *in vivo* pharmacology evaluations of compound **3m** showed significant antitumor activity (TGI = 66.1%) in FGFR-driven NCI-H1581 xenografts with good PK profiles in SD rats and CD-1 mice.The multi-kinase activity of the lead molecule may also account for the observed toxicities in the xenograft, which could be mitigated by structural optimization to remove EGFR WT activity of the future analogs. This novel scaffold of potent protein kinase inhibitors demonstrated a promising prospect for the discovery and development of new NSCLC agents and drugs.

Experimental section

Virtual screening

Protein structure preparation

The protein structure of human FGFR1 in complexed with **15** was downloaded from the Protein Data Bank (PDB code: 3TT0). Protein structure was prepared with the *Protein Preparation Wizard* module in the Maestro program (Maestro, version 10; Schrödinger, LLC: New York, NY, 2015), which includes adding hydrogen atoms, deleting nonstructural water with less than 3 hydrogen bonds to non-waters,

optimizing the hydrogen bond assignment with an exhaustive sampling, optimizing the hydrogen bond network, flip orientations, and tautomeric states of Gln, Asn, and His residues, and finally performing a restrained minimization on the ligand-protein complexes with the OPLS3 force field converged heavy atoms to RMSD of 0.3Å. Specific parameters were set as the default.

Ligand preparation

Our own compound database contained 6,059 structural variety of compounds was used as the ligand database for virtual screening. The ligand database was prepared using LigPrep module in the Shcrödinger software (*LigPrep*, version 3.4; Schrödinger, LLC: New York, NY, 2015) to generate accurate, energy minimized 3D molecular structure. The parameters in LigPrep were set to retain the specific chirality of compounds and generate at most 32 conformations and one lowest energy ring conformation per ligand, in addition, the ionization of compounds were determined at pH 7.0 ± 2.0 by Epik (*Epik*, version 3.2; Schrödinger, LLC: New York, NY, 2015).

Molecular docking

Molecular docking was following the standard Glide protocol. Receptor grid file was generated based on the prepared protein structure. The enclosing box centered at the ligand **15** with size of 18 Å, and extra precision molecular docking was carried out with the receptor grid file and the prepared ligands database. Epik state penalties were added to docking score, and other parameters were used the default settings were used for other parameters. Virtual screening was completed with standard Glide protocol. Altogether 1120 top-ranked poses with XP scores lower than -7.0 kcal/mol were kept.

After removal of the duplicated compounds, the remaining 949 compounds were clustered with the software of BIOVIA Pipeline Pilot (*Pipeline Pilot*, version 7.5, BIOVIA, http://accelrys.com). The molecular fingerprints ECFP4 used for clustering analysis, and the average compound number of each cluster was set to 20. For each cluster, only one or two compounds with higher docking scores were retained and finally 57 compounds were selected for biological evaluation. The putative binding modes of multi-substituted pyridin-3-amine derivatives were all generated using Glide in XP mode with the same procedures described above.

Chemistry. The reagents (chemicals) were purchased and used without further purification. Nuclear magnetic resonance (NMR) spectroscopy was performed on a Bruker AMX-400 and AMX-300 NMR (IS as TMS). Chemical shifts were reported in parts per million (ppm, δ) downfield from tetramethylsilane. Proton coupling patterns were described as singlet (s), doublet (d), triplet (t), quartet (q), multiplet (m), and broad (br). Low- and high-resolution mass spectra (LRMS and HRMS) were given with electric, electrospray, and matrix-assisted laser desorption ionization (EI, ESI, and MALDI) produced by a Finnigan MAT-95, LCQ-DECA spectrometer and IonSpec 4.7 T. Optical rotations were measured using a 1 mL cell with a 10 mm path length on an Auto pol V PLVS matic polarimeter and were reported as follows: $[\alpha]^{20}_{D}$ (c: g/100 mL, in solvent). HPLC analysis of all final biological testing compounds was carried out on an Agilent 1260 Series HPLC with an Agilent Extend-C18 column (150×4.6 mm, 5 μm). All final compounds achieved a minimum of 95% purity.

(*R*)-2-(6-(Furan-3-yl)-5-(3-methyl-1H-indazol-5-yl)pyridin-3-ylamino)-2-phenylet

hanol (1). To (*R*)-2-(6-chloro-5-(3-methyl-1H-indazol-5-yl)pyridin-3-ylamino)-2-phenylethanol **11a** (150 mg, 0.40 mmol), furan-3-ylboronic acid (66 mg, 0.59 mmol) and K_2CO_3(137 mg, 0.99 mmol) in microwave tube, 3 mL of dioxane and 300 μL of water was added, followed by the addition of $Pd(dppf)_2Cl_2 \cdot CH_2Cl_2$ (32 mg, 0.04 mmol). The reaction mixture was filled with argon and was then heated at 120 °C for 2 h under microwave heating. TLC and LC-MS showed the reaction completed. The resulting reaction medium was diluted with DCM (20 mL) and filtered. The filtrate was washed with water (20 mL) by three times and the aqueous layer was re-extracted by DCM (20 mL). The combined organic layer was washed by brine, dried over anhydrous Na_2SO_4 and concentrated under vacuum. The crude product was purified by silica gel column chromatography ($MeOH/CH_2Cl_2$, 1/50 - 1/20) to afford compound **1** as a pale yellow solid (69 mg, 42% yield). ^{1}H NMR (400 MHz, CD_3OD) δ 7.90 (d, *J* = 2.8 Hz, 1H), 7.47 – 7.41 (m, 3H), 7.39 (d, *J* = 8.7 Hz, 1H), 7.35 (t, *J* = 7.5 Hz, 2H), 7.27 (d, *J* = 7.3 Hz, 1H), 7.24 (t, *J* = 1.7 Hz, 1H), 7.12 (d, *J* = 8.6 Hz, 1H), 6.94 (dd, *J* = 1.5, 0.8 Hz, 1H), 6.92 (d, *J* = 2.8 Hz, 1H), 6.15 (dd, *J* = 1.8, 0.8 Hz, 1H), 4.53 (dd, *J* = 7.8, 4.7 Hz, 1H), 3.79 (ddd, *J* = 19.1, 11.2, 6.3 Hz, 2H), 2.51 (s, 3H). ^{13}C NMR (125 MHz, DMSO-d_6) *δ* 142.4, 142.1, 141.4, 140.1, 139.8, 136.8, 135.7, 133.9, 131.6, 128.3(2C), 127.4, 127.1(2C), 127.0, 126.4, 122.3, 121.2, 119.7, 110.6, 109.9, 65.9, 59.1, 11.7. mp 175.3 – 178.2 ^{o}C. $[\alpha]^{20}_{D}$ = -16.5 (c = 0.085 g/100 mL, CH_3OH). LRMS $[M+H]^+$:411.1; HRMS (ESI) cacld for $C_{25}H_{23}N_4O_2$ $[M+H]^+$: 411.1816, Found: 411.1818.

(*R*)-2-(6-(Furan-2-yl)-5-(3-methyl-1H-indazol-5-yl)pyridin-3-ylamino)-2-phenylethanol (2a). Compound **2a** was prepared in a similar manner as described for compound **1**. Yield: 41%; ^{1}H NMR (300 MHz, CD_3OD) δ 7.93 (d, *J* = 2.5 Hz, 1H), 7.45 – 7.39 (m, 4H), 7.36 (d, *J* = 7.3 Hz, 2H), 7.33 – 7.30 (m, 1H), 7.29 – 7.24 (m, 1H), 7.08 (dd, *J* = 8.6, 1.4 Hz, 1H), 6.89 (d, *J* = 2.7 Hz, 1H), 6.20 (dd, *J* = 3.3, 1.8 Hz, 1H), 5.66 (d, *J* = 3.1 Hz, 1H), 4.54 (dd, *J* = 7.7, 4.9 Hz, 1H), 3.79 (ddd, *J* = 19.0, 11.2, 6.3 Hz, 2H), 2.50 (s, 3H). mp 130.8 – 134.1 ^{o}C. $[\alpha]^{20}_D$ = -16.5 (c = 0.085 g/100 mL, CH_3OH). LRMS: $[M+H]^+$:411.1 HRMS (ESI) cacld for $C_{25}H_{23}N_4O_2$ $[M+H]^+$:411.1821, Found: 411.1814.

(*R*)-2-(5-(3-Methyl-1H-indazol-5-yl)-6-(thiophen-3-yl)pyridin-3-ylamino)-2-phenylethanol (2b). Compound **2b** was prepared in a similar manner as described for compound **1**. Yield: 44%; ^{1}H NMR (400 MHz, CD_3OD) δ 7.92 (d, *J* = 2.7 Hz, 1H), 7.44 (d, *J* = 7.2 Hz, 2H), 7.40 – 7.33 (m, 3H), 7.32 – 7.25 (m, 2H), 7.13 (dd, *J* = 5.0, 3.0 Hz, 1H), 7.02 (dd, *J* = 4.3, 1.4 Hz, 1H), 7.00 (t, *J* = 1.3 Hz, 1H), 6.97 (d, *J* = 2.7 Hz, 1H), 6.73 (dd, *J* = 5.0, 1.2 Hz, 1H), 4.56 (dd, *J* = 7.8, 4.7 Hz, 1H), 3.80 (ddd, *J* = 19.1, 11.2, 6.3 Hz, 1H), 2.47 (s, 3H). mp 212.7 – 215.4 ^{o}C. $[\alpha]^{20}_D$ = -26.7 (c = 0.09 g/100 mL, CH_3OH). LRMS $[M+H]^+$: 427.1; HRMS (ESI) cacld for $C_{25}H_{23}N_4OS$ $[M+H]^+$: 427.1587, Found: 427.1589.

(*R*)-2-(5-(3-Methyl-1H-indazol-5-yl)-6-(thiophen-2-yl)pyridin-3-ylamino)-2-phenylethanol (2c). Compound **2c** was prepared in a similar manner as described for compound **1**. Yield: 46%; ^{1}H NMR (400 MHz, DMSO-d_6) δ 7.90 (d, *J* = 2.7 Hz, 1H), 7.44 – 7.39 (m, 3H), 7.36 – 7.31 (m, 3H), 7.28 – 7.24 (m, 1H), 7.15 (dd, *J* = 5.1, 1.1

Hz, 1H), 7.07 (dd, *J* = 8.6, 1.5 Hz, 1H), 6.87 (d, *J* = 2.7 Hz, 1H), 6.68 (dd, *J* = 5.1, 3.7 Hz, 1H), 6.37 (dd, *J* = 3.7, 1.1 Hz, 1H), 4.53 (dd, *J* = 7.8, 4.7 Hz, 1H), 3.78 (ddd, *J* = 19.1, 11.2, 6.3 Hz, 2H), 2.48 (s, 3H). mp 117.6 – 121.3 ^{o}C. $[\alpha]^{20}_{D}$ = -25.0 (c = 0.08 g/100 mL, CH_3OH). LRMS $[M+H]^+$: 427.1; HRMS (ESI) cacld for $C_{25}H_{23}N_4OS$ $[M+H]^+$: 427.1593, Found: 427.1591.

(*R*)-2-(5-(3-Methyl-1H-indazol-5-yl)-6-phenylpyridin-3-ylamino)-2-phenylethanol (2d). Compound **2d** was prepared in a similar manner as described for compound **1**. Yield: 41%; ^{1}H NMR (400 MHz, CD_3OD) δ 7.95 (d, *J* = 2.7 Hz, 1H), 7.46 (d, *J* = 7.1 Hz, 2H), 7.38 (t, *J* = 7.5 Hz, 2H), 7.34 (dd, *J* = 1.5, 0.8 Hz, 1H), 7.29 (t, *J* = 7.3 Hz, 1H), 7.20 (dd, *J* = 8.7, 0.7 Hz, 1H), 7.16 – 7.12 (m, 5H), 7.03 (d, *J* = 2.7 Hz, 1H), 6.93 (dd, *J* = 8.6, 1.6 Hz, 1H), 4.57 (dd, *J* = 7.9, 4.7 Hz, 1H), 3.81 (ddd, *J* = 19.0, 11.2, 6.3 Hz, 2H), 2.44 (s, 3H). ^{13}C NMR (125 MHz, DMSO-d_6) δ 143.9, 143.1, 141.4, 141.2, 140.6, 139.8, 135.7, 134.0, 131.9, 129.3(2C), 128.3(2C), 127.9, 127.4(2C), 127.1(2C), 127.0, 126.2, 122.4, 121.4, 119.9, 109.5, 65.9, 59.8, 11.6. mp 130.3 – 132.7 ^{o}C. $[\alpha]^{20}_{D}$ = -35.6 (c = 0.09 g/100 mL, CH_3OH). LRMS $[M+H]^+$: 421.2; HRMS (ESI) cacld for $C_{27}H_{25}N_4O$ $[M+H]^+$: 421.2023,Found: 421.2022.

(R)-2-(3-(3-Methyl-1H-indazol-5-yl)-2,3'-bipyridin-5-ylamino)-2-phenylethanol (2e). Compound **2e** was prepared in a similar manner as described for compound **1**. Yield: 48%;^{1}H NMR (400 MHz, CD_3OD) δ 8.33 – 8.16 (m, 2H), 8.04 (d, *J* = 2.7 Hz, 1H), 7.67 – 7.58 (m, 1H), 7.45 (d, *J* = 7.3 Hz, 2H), 7.40 – 7.31 (m, 3H), 7.31 – 7.18 (m, 3H), 7.02 (d, *J* = 2.7 Hz, 1H), 6.94 (dd, *J* = 8.6, 1.5 Hz, 1H), 4.59 (dd, *J* = 7.7, 4.7 Hz, 1H), 3.81 (ddd, *J* = 19.1, 11.2, 6.3 Hz, 2H), 2.45 (s, 3H). mp 135.0 – 137.2 ^{o}C.

$[\alpha]^{20}_{D}$ = -43.5 (c = 0.085g/100 mL, CH_3OH). LRMS $[M+H]^+$: 422.2; HRMS (ESI) cacld for $C_{26}H_{24}N_5O$ $[M+H]^+$: 422.1981,Found: 422.1982.

(*R*)-2-(5-(3-Methyl-1H-indazol-5-yl)-6-(quinolin-8-yl)pyridin-3-ylamino)-2-phenylethanol (2f). Compound **2f** was prepared in a similar manner as described for compound **1**. Yield: 46%; ^{1}H NMR (400 MHz, CD_3OD) δ 8.57 (s, 1H), 8.22 (d, *J* = 7.6 Hz, 1H), 8.01 (s, 1H), 7.82 (d, *J* = 7.8 Hz, 1H), 7.55 – 7.43 (m, 4H), 7.41 – 7.32 (m, 3H), 7.28 (t, *J* = 7.3 Hz, 1H), 7.21 (s, 1H), 7.17 (d, *J* = 2.1 Hz, 1H), 6.97 (d, *J* = 8.6 Hz, 1H), 6.89 (dd, *J* = 8.7, 1.4 Hz, 1H), 4.62 (dd, *J* = 7.7, 4.7 Hz, 1H), 3.83 (ddd, *J* = 19.0, 11.2, 6.3 Hz, 2H), 2.25 (s, 3H). mp 160.9 – 163.7 °C. $[\alpha]^{20}_{D}$ = -32.2 (c = 0.09 g/100 mL, CH_3OH). LRMS $[M+H]^+$:472.2; HRMS (ESI) cacld for $C_{30}H_{26}N_5O$ $[M+H]^+$: 472.2137, Found: 472.2126.

(*R*)-2-(6-(1H-Indol-7-yl)-5-(3-methyl-1H-indazol-5-yl)pyridin-3-ylamino)-2-phenylethanol (2g). Compound **2g** was prepared in a similar manner as described for compound **1**. Yield: 38%; ^{1}H NMR (400 MHz, CD_3OD) δ 8.02 (d, *J* = 2.7 Hz, 1H), 7.48 (d, *J* = 7.3 Hz, 2H), 7.42 – 7.33 (m, 4H), 7.29 (t, *J* = 7.3 Hz, 1H), 7.12 (d, *J* = 2.7 Hz, 1H), 7.08 (d, *J* = 3.2 Hz, 1H), 7.06 (d, *J* = 8.7 Hz, 1H), 6.90 (dd, *J* = 8.7, 1.5 Hz, 1H), 6.74 (t, *J* = 7.6 Hz, 1H), 6.64 (dd, *J* = 7.3, 0.9 Hz, 1H), 6.36 (d, *J* = 3.2 Hz, 1H), 4.60 (dd, *J* = 7.9, 4.7 Hz, 1H), 3.82 (ddd, *J* = 19.1, 11.2, 6.3 Hz, 2H), 2.37 (s, 3H). mp 167.3 – 170.8 °C. $[\alpha]^{20}_{D}$ = -54.7 (c = 0.075 g/100 mL, CH_3OH). LRMS $[M+H]^+$: 460.1; HRMS (ESI) cacld for $C_{29}H_{26}N_5O_2$ $[M+H]^+$: 460.2132, Found: 460.2136.

(*R*)-2-(6-(2-Fluorophenyl)-5-(3-methyl-1H-indazol-5-yl)pyridin-3-ylamino)-2-phenylethanol (2h). Compound **2h** was prepared in a similar manner as described for

compound **1**. Yield: 37%; ^{1}H NMR (400 MHz, CD_3OD) δ 7.96 (d, *J* = 2.6 Hz, 1H), 7.45 (d, *J* = 7.3 Hz, 2H), 7.36 (t, *J* = 7.5 Hz, 2H), 7.31 – 7.13 (m, 5H), 7.06 (t, *J* = 7.1 Hz, 1H), 7.03 (d, *J* = 2.7 Hz, 1H), 6.97 (dd, *J* = 8.7, 1.3 Hz, 1H), 6.86 – 6.80 (m, 1H), 4.57 (dd, *J* = 7.7, 4.6 Hz, 1H), 3.81 (ddd, *J* = 19.1, 11.2, 6.3 Hz, 2H), 2.38 (s, 3H). mp 155.1 – 157.6 ^{o}C. $[\alpha]^{20}_D$ = -65.3 (c = 0.095 g/100 mL, CH_3OH). LRMS $[M+H]^+$:439.1; HRMS (ESI) cacld for $C_{27}H_{24}N_4O$ F $[M+H]^+$: 439.1934, Found: 439.1945.

(*R*)-2-(5-(3-Methyl-1H-indazol-5-yl)-6-(2-(trifluoromethyl)phenyl)pyridin-3-ylamino)-2-phenylethanol (2i). Compound **2i** was prepared in a similar manner as described for compound **1**. Yield: 51%; ^{1}H NMR (400 MHz, DMSO-d_6) δ 7.94 (s, 1H), 7.62 (s, 1H), 7.46 (d, *J* = 7.3 Hz, 2H), 7.43 – 7.25 (m, 5H), 7.18 (d, *J* = 8.6 Hz, 2H), 7.14 – 6.85 (m, 3H), 4.57 (dd, *J* = 7.3, 4.8 Hz, 1H), 3.82 (ddd, *J* = 19.1, 11.2, 6.4 Hz, 2H), 2.38 (s, 3H). mp 140.8 – 142.7 ^{o}C. $[\alpha]^{20}_D$ = -46.3 (c = 0.095 g/100 mL, CH_3OH). LRMS $[M+H]^+$:489.1; HRMS (ESI) cacld for $C_{28}H_{24}N_4OF_3$ $[M+H]^+$: 489.1982, Found: 489.1984.

(*R*)-N-(2-(5-(2-Hydroxy-1-phenylethylamino)-3-(3-methyl-1H-indazol-5-yl)pyridin-2-yl)phenyl)acetamide (2j). Compound **2j** was prepared in a similar manner as described for compound **1**. Yield: 48%; ^{1}H NMR (400 MHz, CD_3OD) δ 7.99 (d, *J* = 2.7 Hz, 1H), 7.52 (d, *J* = 8.1 Hz, 1H), 7.46 (d, *J* = 7.3 Hz, 2H), 7.36 (t, *J* = 7.5 Hz,2H), 7.31 – 7.25 (m, 2H), 7.22 – 7.14 (m, 2H), 7.10 (dd, *J* = 7.7, 1.5 Hz, 1H), 7.06 (d, *J* = 2.7 Hz, 1H), 7.01 (t, *J* = 7.5 Hz, 1H), 6.97 (dd, *J* = 8.7, 1.5 Hz, 1H), 4.58 (dd, *J* = 7.9, 4.7 Hz, 1H), 3.81 (ddd, *J* = 19.1, 11.2, 6.3 Hz, 2H), 2.40 (s, 3H), 1.78 (s, 3H). mp 170.3 – 172.9 ^{o}C. $[\alpha]^{20}_D$ = -9.0 (c = 0.1 g/100 mL, CH_3OH). LRMS $[M+H]^+$: 478.2;

HRMS (ESI) cacld for $C_{29}H_{28}N_5O_2$ $[M+H]^+$: 478.2243, Found: 478.2232

(*R*)-2-(6-(2-(Hydroxymethyl)phenyl)-5-(3-methyl-1H-indazol-5-yl)pyridin-3-ylamino)-2-phenylethanol (2k). Compound **2k** was prepared in a similar manner as described for compound **1**. Yield: 49%; ^{1}H NMR (400 MHz, DMSO-d_6) δ 7.94 (d, J = 2.6 Hz, 1H), 7.46 (d, J = 7.4 Hz, 2H), 7.42 – 7.34 (m, 3H), 7.31 – 7.25 (m, 2H), 7.21 (t, J = 7.5 Hz, 1H), 7.15 (d, J = 8.7 Hz, 1H), 7.07 (d, J = 2.6 Hz, 1H), 7.03 (t, J = 7.5 Hz, 1H), 6.96 (d, J = 8.7 Hz, 1H), 6.91 (d, J = 7.6 Hz, 1H), 4.57 (dd, J = 7.7, 4.7 Hz, 1H), 4.28 (s, 2H), 3.81 (ddd, J = 19.1, 11.2, 6.3 Hz, 2H), 2.39 (s, 3H). mp 140.4 – 142.6 ^{o}C. $[\alpha]^{20}_D$ = -52.2 (c = 0.115 g/100 mL, CH_3OH). LRMS $[M+H]^+$: 451.2; HRMS (ESI) cacld for $C_{28}H_{27}N_4O_2$ $[M+H]^+$: 451.2134, Found: 451.2128.

(*R*)-2-(5-(2-Hydroxy-1-phenylethylamino)-3-(3-methyl-1H-indazol-5-yl)pyridin-2-yl)benzamide (2l). Compound **2l** was prepared in a similar manner as described for compound **1**. Yield: 35%; ^{1}H NMR (400 MHz, DMSO-d_6) δ 7.89 (d, J = 2.6 Hz, 1H), 7.49 (dd, J = 7.4, 1.5 Hz, 1H), 7.45 (d, J = 7.2 Hz, 2H), 7.36 (dd, J = 13.9, 6.6 Hz, 3H), 7.30 – 7.19 (m, 3H), 7.16 (d, J = 8.7 Hz, 1H), 7.10 (dd, J = 8.7, 1.5 Hz, 1H), 7.03 (d, J = 2.7 Hz, 1H), 7.00 (dd, J = 7.4, 1.5 Hz, 1H), 4.54 (dd, J = 7.8, 4.7 Hz, 1H), 3.79 (ddd, J = 19.2, 11.2, 6.3 Hz, 2H), 2.39 (s, 3H). mp 216.5 – 219.8 ^{o}C. $[\alpha]^{20}_D$ = -30.5 (c = 0.095 g/100 mL, CH_3OH). LRMS $[M+H]^+$: 464.2; HRMS (ESI) cacld for $C_{28}H_{26}N_5O_2$ $[M+H]^+$: 464.2087, Found: 464.2078.

(*R*)-2-(5-(2-Hydroxy-1-phenylethylamino)-3-(3-methyl-1H-indazol-5-yl)pyridin-2-yl)phenol (2m). Compound **2m** was prepared in a similar manner as described for compound **1**. Yield: 32%; ^{1}H NMR (400 MHz, DMSO-d_6) δ 12.61 (s, 1H), 10.97 (s,

1H), 7.95 (d, *J* = 2.7 Hz, 1H), 7.48 – 7.40 (m, 3H), 7.34 (t, *J* = 7.5 Hz, 2H), 7.29 – 7.18 (m, 2H), 7.01 – 6.91 (m, 3H), 6.78 – 6.67 (m, 2H), 6.64 (d, *J* = 6.5 Hz, 1H), 6.43 (t, *J* = 7.5 Hz, 1H), 5.05 (t, *J* = 5.6 Hz, 1H), 4.55 (dd, *J* = 12.0, 6.3 Hz, 1H), 3.74 – 3.60 (m, 2H), 2.41 (s, 3H). mp 239.3 – 241.9 °C. $[\alpha]^{20}_{D}$ = -26.25 (c = 0.08 g/100 mL, CH_3OH). LRMS $[M+H]^+$: 437.1; HRMS (ESI) cacld for $C_{27}H_{25}N_4O_2$ $[M+H]^+$: 437.1972, Found: 437.1971.

(*R*)-2-(6-(2-Methoxyphenyl)-5-(3-methyl-1H-indazol-5-yl)pyridin-3-ylamino)-2-phenylethanol (2n). Compound **7n** was prepared in a similar manner as described for compound **1**. Yield: 49%; ^{1}H NMR (400 MHz, CD_3OD) δ 7.90 (d, *J* = 2.7 Hz, 1H), 7.47 (d, *J* = 7.3 Hz, 2H), 7.37 (t, *J* = 7.4 Hz, 2H), 7.31 – 7.25 (m, 1H), 7.24 – 7.15 (m, 4H), 7.06 – 6.97 (m, 2H), 6.89 (d, *J* = 7.5 Hz, 1H), 6.69 (d, *J* = 8.2 Hz, 1H), 4.56 (dd, *J* = 7.9, 4.6 Hz, 1H), 3.81 (ddd, *J* = 19.1, 11.2, 6.3 Hz, 2H), 3.23 (s, 3H), 2.37 (s, 3H). mp 151.2 – 152.5 °C. $[\alpha]^{20}_{D}$ = -23.3 (c = 0.09 g/100 mL, CH_3OH). LRMS $[M+H]^+$: 451.2; HRMS (ESI) cacld for $C_{28}H_{27}N_4O_2$ $[M+H]^+$: 451.2129, Found : 451.2127.

(*R*)-3-(5-(2-Hydroxy-1-phenylethylamino)-3-(3-methyl-1H-indazol-5-yl)pyridin-2-yl)phenol (2o). Compound **2o** was prepared in a similar manner as described for compound **1**. Yield: 38%; ^{1}H NMR (400 MHz, DMSO-d_6) δ 12.60 (s, 1H), 9.10 (s, 1H), 7.99 (d, *J* = 2.7 Hz, 1H), 7.46 – 7.40 (m, 3H), 7.33 (t, *J* = 7.5 Hz, 2H), 7.25 (d, *J* = 7.3 Hz, 1H), 7.22 (d, *J* = 8.3 Hz, 1H), 6.89 – 6.81 (m, 3H), 6.66 – 6.61 (m, 1H), 6.53 – 6.43 (m, 3H), 5.02 (t, *J* = 5.6 Hz, 1H), 4.53 (dd, *J* = 12.1, 6.4 Hz, 1H), 3.71 – 3.59 (m, 2H), 2.43 (s, 3H). mp 173.8 – 175.1 °C. $[\alpha]^{20}_{D}$ = -40.0 (c = 0.085 g/100 mL, CH_3OH). LRMS $[M+H]^+$: 437.1; HRMS (ESI) cacld for $C_{27}H_{25}N_4O_2$ $[M+H]^+$:

437.1972, Found: 437.1975.

(*R*)-4-Chloro-2-(5-(2-hydroxy-1-phenylethylamino)-3-(3-methyl-1H-indazol-5-yl) pyridin-2-yl)phenol (2p). Compound **2p** was prepared in a similar manner as described for compound **1**. Yield: 47%; ^{1}H NMR (400 MHz, CD_3OD) δ 7.93 (d, *J* = 2.7 Hz, 1H), 7.45 (d, *J* = 7.2 Hz, 2H), 7.40 – 7.38 (m, 1H), 7.36 (t, *J* = 7.5 Hz, 2H), 7.30 – 7.25 (m, 2H), 7.06 – 7.01 (m, 2H), 6.96 (dd, *J* = 8.7, 2.6 Hz, 1H), 6.79 (d, *J* = 2.6 Hz, 1H), 6.65 (d, *J* = 8.7 Hz, 1H), 4.57 (dd, *J* = 7.8, 4.7 Hz, 1H), 3.81 (ddd, *J* = 19.1, 11.2, 6.3 Hz, 2H), 2.45 (s, 3H). ^{13}C NMR (125 MHz, DMSO-d_6) *δ* 154.7, 143.4, 141.3, 141.3, 140.9, 139.9, 137.0, 132.0, 131.6, 130.0, 128.4, 127.7, 127.1, 127.0, 122.4, 121.9, 121.4, 119.6, 117.6, 109.6, 65.9, 59.1, 11.7. mp 138.7 – 140.1 ^{o}C. $[\alpha]^{20}_D$ = -32.0 (c = 0.075 g/100 mL, CH_3OH). LRMS $[M+H]^+$: 471.1; HRMS(ESI) cacld for $C_{27}H_{24}N_4O_2Cl$ $[M+H]^+$: 471.1582, Found: 471.1580.

(*R*)-4-Chloro-2-(5-(2-hydroxy-1-phenylethylamino)-3-(3-methyl-1H-pyrazolo[3,4-b]pyridin-5-yl)pyridin-2-yl)phenol (3a). Compound **3a** was prepared in a similar manner as described for compound **1**. Yield: 50%; ^{1}H NMR (400 MHz, CD_3OD) δ 8.14 (d, *J* = 1.9 Hz, 1H), 7.99 (d, *J* = 2.7 Hz, 1H), 7.86 (d, *J* = 2.0 Hz, 1H), 7.49 – 7.44 (m, 2H), 7.36 (t, *J* = 7.5 Hz, 2H), 7.28 (t, *J* = 7.3 Hz, 1H), 7.06 – 7.00 (m, 3H), 6.57 (dd, *J* = 7.4, 1.6 Hz, 1H), 4.59 (dd, *J* = 7.8, 4.8 Hz, 1H), 3.82 (ddd, *J* = 19.1, 11.2, 6.3 Hz, 2H), 2.46 (s, 3H). ^{13}C NMR (125 MHz, DMSO-d_6) *δ* 153.7, 151.3, 148.6, 143.5, 141.3, 141.2, 141.0, 134.0, 133.4, 130.5, 128.5, 128.4, 128.3(2C), 128.0, 127.1(3C), 121.8, 120.8, 117.2, 113.5, 65.9, 59.0, 12.1. mp 142.9 – 145.0 ^{o}C. $[\alpha]^{20}_D$ = -21.3 (c = 0.075 g/100 mL, CH_3OH). LRMS $[M+H]^+$:472.1; HRMS(ESI) cacld for

$C_{26}H_{23}N_5O_2Cl$ $[M+H]^+$: 472.1535, Found: 472.1538.

(*R*)-4-Chloro-2-(5-(2-hydroxy-1-phenylethylamino)-3-(isoquinolin-6-yl)pyridin-2-yl)phenol (3b). Compound **3b** was prepared in a similar manner as described for compound **1**. Yield: 53%; ^{1}H NMR (400 MHz, CD_3OD) δ 9.15 (s, 1H), 8.38 (d, *J* = 5.8 Hz, 1H), 8.00 (d, *J* = 2.7 Hz, 1H), 7.92 (d, *J* = 8.6 Hz, 1H), 7.68 (d, *J* = 6.8 Hz, 2H), 7.49 – 7.42 (m, 2H), 7.40 – 7.32 (m, 3H), 7.27 (t, *J* = 7.3 Hz, 1H), 7.08 (d, *J* = 2.7 Hz, 1H), 6.98 (dd, *J* = 8.7, 2.6 Hz, 1H), 6.91 (d, *J* = 2.6 Hz, 1H), 6.59 (d, *J* = 8.7 Hz, 1H), 4.63 – 4.57 (m, 1H), 3.81 (ddd, *J* = 19.1, 1.2, 6.3 Hz, 2H). mp 124.9 – 127.5 ^{o}C. $[\alpha]^{20}_D$ = -48.0 (c = 0.075 g/100 mL, CH_3OH). LRMS $[M+H]^+$: 468.1; HRMS (ESI) cacld for $C_{28}H_{23}N_3O_2Cl$ $[M+H]^+$: 468.1473, Found: 468.1477.

(*R*)-5-(2-(5-Chloro-2-hydroxyphenyl)-5-(2-hydroxy-1-phenylethylamino)pyridin-3-yl)indolin-2-one (3c). Compound **3c** was prepared in a similar manner as described for compound **1**. Yield: 46%; ^{1}H NMR (400 MHz, DMSO-d_6) δ 10.75 (s, 1H), 10.40 (s, 1H), 7.94 (d, *J* = 2.4 Hz, 1H), 7.42 (d, *J* = 7.4 Hz, 2H), 7.33 (t, *J* = 7.5 Hz, 2H), 7.23 (t, *J* = 7.1 Hz, 1H), 7.02 (dd, *J* = 8.7, 2.6 Hz, 1H), 6.97 (s, 1H), 6.86 (d, *J* = 2.8 Hz, 2H), 6.82 (d, *J* = 2.6 Hz, 1H), 6.72 – 6.62 (m, 3H), 5.03 (t, *J* = 5.5 Hz, 1H), 4.53 (dd, *J* = 12.1, 6.3 Hz, 1H), 3.70 – 3.59 (m, 2H), 3.40 (s, 2H). mp 126.1 – 128.5 ^{o}C. $[\alpha]^{20}_D$ = -15.2 (c = 0.105 g/100 mL, CH_3OH). LRMS $[M+H]^+$: 472.1; HRMS (ESI) cacld for $C_{27}H_{23}N_3O_3Cl$ $[M+H]^+$: 472.1422, Found: 472.1420.

(*R*)-*N*-(4-(2-(5-Chloro-2-hydroxyphenyl)-5-(2-hydroxy-1-phenylethylamino)pyridin-3-yl)phenyl)acetamide (3d). Compound **3d** was prepared in a similar manner as described for compound **1**. Yield: 61%; ^{1}H NMR (400 MHz, CD_3OD) δ 7.90 (d, *J* =

2.7 Hz, 1H), 7.46 – 7.41 (m, 4H), 7.35 (t, *J* = 7.5 Hz, 2H), 7.27 (t, *J* = 7.3 Hz, 1H), 7.04 – 6.97 (m, 3H), 6.95 (d, *J* = 2.7 Hz, 1H), 6.82 (d, *J* = 2.6 Hz, 1H), 6.67 (d, *J* = 8.7 Hz, 1H), 4.55 (dd, *J* = 7.9, 4.7 Hz, 1H), 3.79 (ddd, *J* = 19.1, 11.2, 6.3 Hz, 2H), 2.11 (s, 3H). mp 129.0 – 130.2 ^{o}C. $[\alpha]^{20}_{D}$ = -28.0 (c = 0.1 g/100 mL, CH_3OH). LRMS $[M-H]^+$: 472.1; HRMS (ESI) cacld for $C_{27}H_{23}N_3O_3Cl$ $[M-H]^+$: 472.1433, Found: 472.1442.

(*R*)-4-Chloro-2-(5-(2-hydroxy-1-phenylethylamino)-3-(1H-indol-5-yl)pyridin-2-yl)phenol (3e). Compound **3e** was prepared in a similar manner as described for compound **1**. Yield: 53%; ^{1}H NMR (400 MHz, CD_3OD) δ 7.88 (d, *J* = 2.7 Hz, 1H), 7.44 (d, *J* = 7.2 Hz, 2H), 7.35 (t, *J* = 7.5 Hz, 2H), 7.31 (d, *J* = 1.2 Hz, 1H), 7.29 – 7.22 (m, 2H), 7.22 (d, *J* = 3.1 Hz, 1H), 7.04 (d, *J* = 2.7 Hz, 1H), 6.91 (dd, *J* = 8.7, 2.6 Hz, 1H), 6.78 (dd, *J* = 8.4, 1.6 Hz, 1H), 6.73 (d, *J* = 2.6 Hz, 1H), 6.67 (d, *J* = 8.7 Hz, 1H), 6.38 (dd, *J* = 3.1, 0.7 Hz, 1H), 4.56 (dd, *J* = 7.7, 4.8 Hz, 1H), 3.80 (ddd, *J* = 19.1, 11.2, 6.3 Hz, 2H). mp 116.7 – 121.5 ^{o}C. $[\alpha]^{20}_{D}$ = -37.0 (c = 0.1 g/100 mL, CH_3OH). LRMS $[M+H]^+$: 456.1; HRMS (ESI) cacld for $C_{27}H_{23}N_3O_2Cl$ $[M+H]^+$: 456.1473, Found: 456.1470.

(*S*)-4-Chloro-2-(5-(2-hydroxy-1-phenylethylamino)-3-(3-methyl-1H-indazol-5-yl) pyridin-2-yl)phenol (3f). Compound **3f** was prepared in a similar manner as described for compound **1**. Yield: 46%; ^{1}H NMR (400 MHz, CD_3OD) δ 7.93 (d, *J* = 2.7 Hz, 1H), 7.45 (d, *J* = 7.7 Hz, 2H), 7.42 – 7.32 (m, 3H), 7.31 – 7.23 (m, 2H), 7.03 (dd, *J* = 10.5, 2.1 Hz, 2H), 6.96 (dd, *J* = 8.7, 2.6 Hz, 1H), 6.79 (d, *J* = 2.6 Hz, 1H), 6.64 (d, *J* = 8.7 Hz, 1H), 4.56 (dd, *J* = 7.7, 4.8 Hz, 1H), 3.80 (ddd, *J* = 19.1, 11.2, 6.3

Hz, 2H), 2.45 (s, 3H). mp 136.5 – 139.1 °C. $[\alpha]^{20}_{D}$ = +28.3 (c = 0.06 g/100 mL, CH_3OH). LRMS $[M+H]^+$: 471.1; HRMS (ESI) cacld for $C_{27}H_{24}N_4O\ _2Cl$ $[M+H]^+$: 471.1588, Found: 471.1578.

(*S*)-4-Chloro-2-(3-(3-methyl-1H-indazol-5-yl)-5-(1-phenylethylamino)pyridin-2-yl)phenol (3g). Compound **8g** was prepared in a similar manner as described for compound **1**. Yield: 52%; ^{1}H NMR (400 MHz, CD_3OD) δ 7.87 (d, *J* = 2.7 Hz, 1H), 7.40 (d, *J* = 7.2 Hz, 2H), 7.36 (d, *J* = 0.6 Hz, 1H), 7.32 (t, *J* = 7.6 Hz, 2H), 7.26 (dd, *J* = 8.6, 0.6 Hz, 1H), 7.22 (t, *J* = 7.3 Hz, 1H), 7.01 (dd, *J* = 8.7, 1.6 Hz, 1H), 6.97 – 6.90 (m, 2H), 6.77 (d, *J* = 2.6 Hz, 1H), 6.64 (d, *J* = 8.7 Hz, 1H), 4.56 (q, *J* = 6.7 Hz, 1H), 2.44 (s, 3H), 1.54 (d, *J* = 6.8 Hz, 3H). mp 107.3 – 109.0 °C. $[\alpha]^{20}_{D}$ = +23.2 (c = 0.095 g/100 mL, CH_3OH). LRMS $[M+H]^+$: 455.1; HRMS (ESI) cacld for $C_{27}H_{24}N_4OCl$ $[M+H]^+$: 455.1639,Found: 455.1627.

(*R*)-4-Chloro-2-(5-(2-hydroxyethylamino)-3-(3-methyl-1H-indazol-5-yl)pyridin-2-yl)phenol (3h). Compound **3h** was prepared in a similar manner as described for compound **1**. Yield: 52%; ^{1}H NMR (400 MHz, CD_3OD) δ 8.01 (d, *J* = 2.7 Hz, 1H), 7.62 (s, 1H), 7.34 (d, *J* = 8.6 Hz, 1H), 7.19 (d, *J* = 8.7 Hz, 1H), 7.15 (d, *J* = 2.7 Hz, 1H), 6.75 (td, *J* = 8.4, 3.0 Hz, 1H), 6.69 (dd, *J* = 8.8, 5.0 Hz, 1H), 6.57 (dd, *J* = 9.8, 3.0 Hz, 1H), 3.78 (t, *J* = 5.7 Hz, 2H), 3.35 (t, *J* = 5.7 Hz, 2H), 2.50 (s, 3H). mp 226.5 – 227.8 °C. LRMS:$[M+H]^+$:379. HRMS (ESI) cacld for $C_{21}H_{20}N_4O_2F$ $[M+H]^+$:379.1565, Found : 379.1566.

(*R*)-4-Chloro-2-(5-(3-hydroxypropylamino)-3-(3-methyl-1H-indazol-5-yl)pyridin-2-yl)phenol (3i). Compound **3i** was prepared in a similar manner as described for

compound **1**. Yield: 54%; ^{1}H NMR (400 MHz, CD_3OD) δ 7.99 (d, *J* = 2.8 Hz, 1H), 7.62 (s, 1H), 7.35 (d, *J* = 8.6 Hz, 1H), 7.19 (dd, *J* = 8.6, 1.5 Hz, 1H), 7.11 (d, *J* = 2.8 Hz, 1H), 6.74 (dd, *J* = 8.0, 3.1 Hz, 1H), 6.72 – 6.66 (m, 1H), 6.56 (dd, *J* = 9.8, 3.0 Hz, 1H), 3.72 (t, *J* = 6.2 Hz, 2H), 2.50 (s, 3H), 1.89 (dd, *J* = 13.1, 6.6 Hz, 2H). mp 249.6 – 252.3 ^{o}C. LRMS $[M+H]^+$: 393.2; HRMS (ESI) cacld for $C_{22}H_{22}N_4O_2F$ $[M+H]^+$: 393.1721, Found: 393.1721.

(*R*)-4-Chloro-2-(5-(2-hydroxy-2-phenylethylamino)-3-(3-methyl-1H-indazol-5-yl) pyridin-2-yl)phenol (3j). Compound **3j** was prepared in a similar manner as described for compound **1**. Yield: 44%; ^{1}H NMR (400 MHz, CD_3OD) δ 7.98 (d, *J* = 2.7 Hz, 1H), 7.57 (s, 1H), 7.44 (d, *J* = 7.2 Hz, 2H), 7.34 (t, *J* = 7.6 Hz, 3H), 7.26 (s, 1H), 7.14 (dd, *J* = 8.6, 1.5 Hz, 1H), 7.08 (d, *J* = 2.7 Hz, 1H), 6.97 (dd, *J* = 8.7, 2.6 Hz, 1H), 6.82 (d, *J* = 2.6 Hz, 1H), 6.67 (d, *J* = 8.7 Hz, 1H), 3.50 – 3.39 (m, 2H), 2.49 (s, 3H). mp 156.7 – 159.3 ^{o}C. $[\alpha]^{20}_D$ = +20.9 (c = 0.11 g/100 mL, CH_3OH). LRMS $[M+H]^+$: 471.1; HRMS (ESI) cacld for $C_{27}H_{24}N_4O_2Cl$ $[M+H]^+$: 471.1588, Found: 471.1586.

(*R*)-2-(5-(2-Hydroxy-1-phenylethylamino)-3-(3-methyl-1H-indazol-5-yl)pyridin-2 -yl)-4-methylphenol (3k). Compound **3k** was prepared in a similar manner as described for compound **1**. Yield: 42%; ^{1}H NMR (400 MHz, CD_3OD) δ 7.91 (d, *J* = 2.7 Hz, 1H), 7.45 (d, *J* = 7.4 Hz, 2H), 7.41 – 7.32 (m, 3H), 7.27 (t, *J* = 7.3 Hz, 1H), 7.22 (d, *J* = 8.6 Hz, 1H), 7.07 – 7.00 (m, 2H), 6.81 (dd, *J* = 8.2, 2.2 Hz, 1H), 6.63 (d, *J* = 1.9 Hz, 1H), 6.57 (d, *J* = 8.2 Hz, 1H), 4.56 (dd, *J* = 7.8, 4.7 Hz, 1H), 3.80 (ddd, *J* = 19.1, 11.2, 6.3 Hz, 2H), 2.43 (s, 3H), 1.92 (s, 3H). mp 93.2 – 95.0 ^{o}C. $[\alpha]^{20}_D$ = -15.6 (c

= 0.09 g/100 mL, CH_3OH). LRMS $[M+H]^+$: 451.2; HRMS (ESI) cacld for $C_{28}H_{27}N_4O_2$ $[M+H]^+$: 451.2134, Found: 451.2123.

(*R*)-2-(5-(2-Hydroxy-1-phenylethylamino)-3-(3-methyl-1H-indazol-5-yl)pyridin-2-yl)-4-isopropylphenol (3l). Compound **3l** was prepared in a similar manner as described for compound **1**. Yield: 31%; ^{1}H NMR (400 MHz, CD_3OD) δ 7.92 (d, *J* = 2.1 Hz, 1H), 7.45 (d, *J* = 7.4 Hz, 2H), 7.38 – 7.33 (m, 3H), 7.28 (d, *J* = 8.1 Hz, 2H), 7.08 – 7.01 (m, 2H), 6.82 (d, *J* = 8.0 Hz, 1H), 6.63 (d, *J* = 8.3 Hz, 1H), 6.58 (s, 1H), 4.56 (dd, *J* = 7.3, 4.8 Hz, 1H), 3.80 (ddd, *J* = 19.0, 11.1, 6.4 Hz, 2H), 2.44 – 2.35 (m, 4H), 0.73 (dd, *J* = 6.7, 4.0 Hz, 6H). mp 128.6 – 131.6 ^{o}C. $[\alpha]^{20}_D$ = -18.8 (c = 0.08 g/100 mL, CH_3OH). LRMS $[M+H]^+$:479.2; HRMS (ESI) cacld for $C_{30}H_{31}N_4O_2$ $[M+H]^+$: 479.2442, Found: 479.2443.

(*R*)-4-Fluoro-2-(5-(2-hydroxy-1-phenylethylamino)-3-(3-methyl-1H-indazol-5-yl) pyridin-2-yl)phenol (3m). Compound **3m** was prepared in a similar manner as described for compound **1**. Yield: 46%; ^{1}H NMR (400 MHz, DMSO-d_6) δ 12.65 (s, 1H), 10.73 (s, 1H), 7.99 – 7.92 (m, 1H), 7.44 (d, *J* = 7.2 Hz, 3H), 7.34 (t, *J* = 7.5 Hz, 2H), 7.29 (d, *J* = 8.7 Hz, 1H), 7.25 (t, *J* = 7.3 Hz, 1H), 6.99 – 6.94 (m, 2H), 6.80 (td, *J* = 8.5, 3.2 Hz, 1H), 6.70 (d, *J* = 6.5 Hz, 1H), 6.65 (dd, *J* = 8.9, 5.1 Hz, 1H), 6.49 (dd, *J* = 10.2, 3.1 Hz, 1H), 5.05 (t, *J* = 5.6 Hz, 1H), 4.56 (dd, *J* = 12.1, 6.4 Hz, 1H), 3.67 (dt, *J* = 12.0, 6.0 Hz, 2H), 2.42 (s, 3H). ^{13}C NMR (125 MHz, CD_3OD) *δ* 157.8, 155.9, 153.3, 145.0, 143.7, 143.4 141.7, 139.1, 133.5, 133.4, 129.8, 129.5, 128.6, 128.2, 127.1 (d, *J* = 7.5 Hz), 124.2, 123.5, 121.3, 118.0 (d, *J* = 12.1 Hz), 117.9 (d, *J* = 3.7 Hz), 115.8 (d, *J* = 23.1 Hz), 110.7, 67.7, 61.2, 11.6. mp 144.5 – 147.9 ^{o}C. $[\alpha]^{20}_D$ =

-27.4 (c = 0.095 g/100 mL, CH_3OH). LRMS $[M+H]^+$: 455.2; HRMS(ESI) cacld for $C_{27}H_{24}N_4O_2F$ $[M+H]^+$: 455.1878, Found: 455.1877.

(*R*)-5-Fluoro-2-(5-(2-hydroxy-1-phenylethylamino)-3-(3-methyl-1H-indazol-5-yl) pyridin-2-yl)phenol (3n). Compound **3n** was prepared in a similar manner as described for compound **1**. Yield: 44%; ^{1}H NMR (400 MHz, CD_3OD) δ 7.92 (d, *J* = 2.7 Hz, 1H), 7.46 (d, *J* = 7.4 Hz, 2H), 7.40 – 7.34 (m, 3H), 7.31 – 7.24 (m, 2H), 7.07 – 7.01 (m, 2H), 6.78 (dd, *J* = 8.2, 7.1 Hz, 1H), 6.43 (dd, *J* = 10.6, 2.6 Hz, 1H), 6.25 (td, *J* = 8.6, 2.2 Hz, 1H), 4.57 (dd, *J* = 7.8, 4.7 Hz, 1H), 3.81 (ddd, *J* = 19.1, 11.2, 6.3 Hz, 2H), 2.46 (s, 3H). mp 140.8 – 143.1 ^{o}C. $[\alpha]^{20}_D$ = -25.5 (c = 0.11 g/100 mL, CH_3OH). LRMS $[M+H]^+$: 455.1; HRMS (ESI) cacld for $C_{27}H_{24}N_4O_2F$ $[M+H]^+$: 455.1878, Found: 455.1883.

(*R*)-2-Fluoro-6-(5-(2-hydroxy-1-phenylethylamino)-3-(3-methyl-1H-indazol-5-yl) pyridin-2-yl)phenol (3o). Compound **3o** was prepared in a similar manner as described for compound **1**. Yield: 39%; ^{1}H NMR (400 MHz, CD_3OD) δ 7.94 (d, *J* = 2.7 Hz, 1H), 7.46 (d, *J* = 7.2 Hz, 2H), 7.40 – 7.35 (m, 3H), 7.29 (d, *J* = 7.3 Hz, 1H), 7.25 (d, *J* = 8.6 Hz, 1H), 7.07 – 7.01 (m, 2H), 6.87 (ddd, *J* = 10.8, 8.1, 1.5 Hz, 1H), 6.62 (d, *J* = 7.8 Hz, 1H), 6.48 (td, *J* = 8.0, 5.0 Hz, 1H), 4.58 (dd, *J* = 7.8, 4.7 Hz, 1H), 3.81 (ddd, *J* = 19.1, 11.2, 6.3 Hz, 2H), 2.45 (s, 3H). mp 135.6 – 138.3 ^{o}C. $[\alpha]^{20}_D$ = -32.3 (c = 0.065 g/100 mL, CH_3OH). LRMS $[M-H]^+$: 453.2; HRMS (ESI) cacld for $C_{27}H_{22}N_4O_2F$ $[M-H]^+$: 453.1732, Found: 453.1739.

(*R*)-4,5-Difluoro-2-(5-(2-hydroxy-1-phenylethylamino)-3-(3-methyl-1H-indazol-5-yl)pyridin-2-yl)phenol (3p). Compound **3p** was prepared in a similar manner as

described for compound **1**. Yield: 40%; ^{1}H NMR (400 MHz, CD_3OD) δ 7.93 (d, *J* = 2.7 Hz, 1H), 7.48 – 7.40 (m, 3H), 7.37 (t, *J* = 7.6 Hz, 2H), 7.34 – 7.26 (m, 2H), 7.04 (dd, *J* = 8.6, 1.5 Hz, 1H), 7.02 (d, *J* = 2.7 Hz, 1H), 6.65 (dd, *J* = 11.9, 9.3 Hz, 1H), 6.55 (dd, *J* = 12.1, 7.1 Hz, 1H), 4.57 (dd, *J* = 7.8, 4.7 Hz, 1H), 3.81 (ddd, *J* = 19.1, 11.3, 6.3 Hz, 2H), 2.48 (s, 3H). mp 146.8 – 149.2 °C. $[\alpha]^{20}_D$ = -23.8 (c = 0.08 g/100 mL, CH_3OH). LRMS $[M+H]^+$: 473.2; HRMS (ESI) cacld for $C_{27}H_{23}N_4O_2F_2$ $[M+H]^+$: 473.1784, Found: 473.1781.

(*R*)-2,4-Difluoro-6-(5-(2-hydroxy-1-phenylethylamino)-3-(3-methyl-1H-indazol-5-yl)pyridin-2-yl)phenol (3q). Compound **3q** was prepared in a similar manner as described for compound **1**. Yield: 37%; ^{1}H NMR (400 MHz, CD_3OD) δ 7.97 (d, *J* = 2.7 Hz, 1H), 7.51 – 7.46 (m, 2H), 7.43 (dd, *J* = 1.5, 0.8 Hz, 1H), 7.39 (t, *J* = 7.5 Hz, 2H), 7.34 – 7.28 (m, 2H), 7.07 (dd, *J* = 8.6, 1.6 Hz, 1H), 7.05 (d, *J* = 2.7 Hz, 1H), 6.80 – 6.73 (m, 1H), 6.41 (ddd, *J* = 9.6, 3.0, 1.9 Hz, 1H), 4.60 (dd, *J* = 7.9, 4.8 Hz, 1H), 3.83 (ddd, *J* = 19.1, 11.2, 6.3 Hz, 2H), 2.49 (s, 3H). mp 143.5 – 145.2 °C. $[\alpha]^{20}_D$ = -24.3(c = 0.09 g/100 mL, CH_3OH). LRMS $[M-H]^+$: 471.1; HRMS (ESI) cacld for $C_{27}H_{21}N_4O_2F_2$ $[M-H]^+$: 471.1638, Found: 471.1646.

1-(5-Bromo-2-fluorophenyl)ethanone (5a). To a stirred solution of 5-bromo-2-fluoro-benzaldehyde (8.00 g, 39.4 mmol) in anhydrous ether (150 mL) under argon atmosphere at 0 °C was added MeMgBr (17.1 mL, 3.0 M solution in ether, 51.2 mmol) slowly. After 1 hour, water was slowly added to the reaction mixture, followed by 1M HCl, under ice bath. The mixture was extracted with EA (200 mL) by three times. The combined organic layer was washed by brine, dried

over anhydrous Na_2SO_4 and concentrated under vacuum. The obtained oil was mixed with dioxane (100 mL), followed by the addition of manganese dioxide (17.13 g, 197.0 mmol). The reaction mixture was heated at reflux for 4 h. The resulting mixture was cooled to room temperature and filtered. The filtrate was concentrated under vacuum and purified by silica gel column chromatography (EA/PE, 1/20 - 1/10) to afford **5a** (6.32g, 74%). ^{1}H NMR (400 MHz, DMSO-d_6) δ 7.92 (dd, J = 6.4, 2.7 Hz, 1H), 7.72 (ddd, J = 8.7, 4.2, 2.7 Hz, 1H), 7.19 (dd, J = 10.7, 8.8 Hz, 1H), 2.59 (d, J = 4.7 Hz, 3H). LRMS $[M+H]^+$: 217.0.

1-(5-Bromo-2-fluoropyridin-3-yl)ethanone (5b). Compound **5b** was prepared in a similar manner as described for compound **10a.** Yield: 71%. LRMS $[M+H]^+$: 218.1.

5-bromo-3-methyl-1H-indazole (6a). To a solution of hydrazine monohydrate (15 mL) was added 1-(5-bromo-2-fluorophenyl)ethanone **10a** (3.0 g, 13.82 mmol). The resulting mixture was refluxed for 24h and then cooled to room temperature. The mixture was poured over ice and the pale brown solid was precipitated. The solid was collected by filtration and purified by silica gel column chromatography (EA/PE, 1/4 - 1/2) to afford **11a** (1.89 g, 65%). ^{1}H NMR (400 MHz, CD_3OD) δ 7.87 (s, 1H), 7.44 (dd, J = 8.8, 1.3 Hz, 1H), 7.39 (d, J = 8.7 Hz, 1H), 2.52 (s, 3H). LRMS $[M+H]^+$: 211.1.

5-Bromo-3-methyl-1H-pyrazolo[3,4-b]pyridine (6b). Compound **6b** was prepared in a similar manner as described for compound **6a.** Yield: 59%; ^{1}H NMR (400 MHz, CD_3OD) δ 8.50 (d, J = 2.1 Hz, 1H), 8.37 (d, J = 2.1 Hz, 1H), 2.52 (s, 3H). LRMS $[M+H]^+$: 212.1.

***Tert*-butyl-3-methyl-5-(4,4,5,5-tetramethyl-1,3,2-dioxaborolan-2-yl)-1H-indazole-1-carboxylate (7a).** To a stirred mixture of 5-bromo-3-methyl-1H-indazole **6a** (2.0 g, 9.48 mmol) and triethylamine (2.0 mL, 14.21 mmol) in THF (20 mL) was added Boc_2O (3.10 g, 14.21 mmol) and DMAP (116 mg, 0.95 mmol) at room temperature. After 4 hours, TLC showed the reaction completed. The resulting mixture was diluted with EA (40 mL) and washed by saturated aqueous citric acid (40 mL) by two times. The organic phase was washed by brine, dried over anhydrous Na_2SO_4 and concentrated under vacuum. The obtained solid was added to the mixture of 4,4,4',4',5,5,5',5'-octamethyl-2,2'-bi(1,3,2-dioxaborolane) (3.61 g, 14.21 mmol) and KOAc (2.33 g, 23.69 mmol) in dioxane (20 mL). The reaction vessel was evacuated and refilled with nitrogen (3 times), followed by the addition of $Pd(dppf)_2Cl_2 \cdot CH_2Cl_2$ (32 mg, 0.04 mmol). The resulting mixture was stirred at 80 °C for 6 h and then cooled to room temperature. The mixture was diluted with EA (30 mL) and filtrated. The filtrate was sequentially washed by water, brine and dried over anhydrous Na_2SO_4. The obtained organic solution was concentrated under vacuum and purified by silica gel column chromatography (EA/PE, 1/15- 1/10) to afford compound **7a** as a white solid (2.17g, 64% yield). ^1H NMR (400 MHz, $CDCl_3$) δ 8.15 (s, 1H), 8.09 (d, J = 8.3 Hz, 1H), 7.93 (dd, J = 8.4, 0.9 Hz, 1H), 2.61 (s, 3H), 1.71 (s, 9H), 1.37 (s, 12H). LRMS $[M+H]^+$: 359.2.

***Tert*-butyl 3-methyl-5-(4,4,5,5-tetramethyl-1,3,2-dioxaborolan-2-yl)-1H-pyrazolo[3,4-b]pyridine-1-carboxylate (7b).** Compound **7b** was prepared in a similar manner as

described for compound **6a.** Yield: 51%; LRMS $[M+H]^+$: 360.1.

3-Bromo-2-chloro-5-iodopyridine (9). To a solution of 5N aqueous HCl (100 mL) were added 5-bromo-6-chloropyridin-3-amine (15 g, 72.30 mmol) and then cooled to 0 °C. An aqueous of $NaNO_2$ (7.48 g, 108.5 mmol) was dropwise added to the former stirred mixture under the ice bath. After 1 hour, to the reaction mixture was very slowly added an aqueous solution of KI (26.41 g, 159.1 mmol) under ice bath. The temperature restored to room temperature gradually, followed by continuing stirring until no generation of nitrogen was observed. Thereafter, the solution was alkalized with sodium hydroxide under ice bath, until pH reached 10-11. The aqueous layer was then extracted with EA (300 mL) by two times. The organic layer was washed with saturated aqueous sodium thiosulfate and brine, which was then dried over anhydrous Na_2SO_4 and concentrated under vacuum. The crude product was purified by silica gel column chromatography (EA/PE, 0 – 1/50) to afford compound **9** as a white solid (20.5 g, 89% yield). ^{1}H NMR (400 MHz, DMSO-d_6) δ 8.68 (d, J = 2.0 Hz, 1H), 8.67 (d, J = 2.0 Hz, 1H). LRMS:$[M+H]^+$:319.9.

(*R*)-2-(5-Bromo-6-chloropyridin-3-ylamino)-2-phenylethanol (10). To a stirred mixture of (*R*)-2-amino-2-phenylethanol (1.24 g, 9.05 mmol) and K_3PO_4 (3.20 g, 15.08 mmol) in isopropanol (20 mL) was added 3-bromo-2-chloro-5-iodopyridine **9** (2.4 g, 7.54 mmol) and ethane-1,2-diol (0.385 mL, 7.54 mmol). The reaction vessel was evacuated and refilled with nitrogen (3 times), followed by the addition of CuI (144 mg, 0.75 mmol). The resulting mixture was stirred at 80 °C for 18 h and then cooled to room temperature. The mixture was diluted with EA (30 mL) and filtrated.

The filtrate was sequentially washed by water, brine and dried over anhydrous Na_2SO_4. The obtained organic solution was concentrated under vacuum and purified by silica gel column chromatography (EA/PE, 1/4- 1/2) to afford compound **10** as a yellow solid (1.31 g, 53% yield). ^{1}H NMR (400 MHz, DMSO-d_6) δ 7.73 (d, J = 2.5 Hz, 1H), 7.37 (d, J = 7.2 Hz, 2H), 7.33 (t, J = 7.5 Hz, 2H), 7.29 – 7.21 (m, 2H), 6.87 (d, J = 6.9 Hz, 1H), 5.06 (t, J = 5.4 Hz, 1H), 4.47 (dd, J = 11.8, 7.0 Hz, 1H), 3.72 – 3.51 (m, 2H). LRMS $[M+H]^+$: 328.9.

(*R*)-2-(6-Chloro-5-(3-methyl-1H-indazol-5-yl)pyridin-3-ylamino)-2-phenylethanol (11a). To a stirred mixture of (*R*)-2-(5-bromo-6-chloropyridin-3-ylamino)-2-phenylethanol **15** (3.0 g, 9.16 mmol) and Na_2CO_3 (2.43 g, 22.89 mmol) in dioxane (50 mL) was added tert-butyl 3-methyl-5-(4,4,5,5-tetramethyl-1,3,2-dioxaborolan-2-yl) -1H-indazole-1-carboxylate **12a** (4.92 g, 13.74 mmol) and 2.5 mL of water. The reaction vessel was evacuated and refilled with nitrogen (3 times), followed by the addition of $Pd(dppf)_2Cl_2 \cdot CH_2Cl_2$ (748 mg, 0.92 mmol). The resulting mixture was stirred at 80 °C overnight and then cooled to room temperature. The mixture was diluted with EA (30 mL) and filtrated. The filtrate was sequentially washed by water, brine and dried over anhydrous Na_2SO_4. The obtained organic solution was concentrated under vacuum. The obtained solid was re-dissolved in DCM (30 mL). To the stirred mixture was added 15 mL of TFA. After 6 hours, the mixture was concentrated under vacuum and neutralized with 1M aqueous sodium hydroxide under ice bath. The mixture was extracted with DCM (65 mL) by three times. The combined organic layer was washed with brine and dried

over anhydrous Na_2SO_4. The obtained solution was concentrated under vacuum and purified by silica gel column chromatography (MeOH/DCM, 1/100- 1/50) to afford compound **11a** as a yellow solid (1.89 g, 55% yield). ^{1}H NMR (400 MHz, CD_3OD) δ 7.66 (d, *J* = 2.9 Hz, 1H), 7.53 (d, *J* = 0.6 Hz, 1H), 7.45 (d, *J* = 8.6 Hz, 1H), 7.42 – 7.37 (m, 2H), 7.36 – 7.30 (m, 3H), 7.26 (t, *J* = 7.2 Hz, 1H), 6.99 (d, *J* = 2.9 Hz, 1H), 4.48 (dd, *J* = 7.8, 4.7 Hz, 1H), 3.77 (ddd, *J* = 19.1, 11.2, 6.3 Hz, 2H), 2.55 (d, *J* = 12.5 Hz, 3H). LRMS $[M+H]^+$: 379.1.

(*R*)-2-(6-Chloro-5-(3-methyl-1H-pyrazolo[3,4-b]pyridin-5-yl)pyridin-3-ylamino)-2-phenylethanol (**11b**). Yield: 48%; Compound **11b** was prepared in a similar manner as described for compound **11a.** LRMS $[M+H]^+$: 380.1.

(*R*)-2-(6-chloro-5-(isoquinolin-6-yl)pyridin-3-ylamino)-2-phenylethanol (12a). To a stirred mixture of (*R*)-2-(5-bromo-6-chloropyridin-3-ylamino)-2-phenylethanol **10** (2.5 g, 7.63 mmol) and K_2CO_3 (2.64 g, 19.08 mmol) in dioxane (30 mL) was added 6-(4,4,5,5-tetramethyl-1,3,2-dioxaborolan-2-yl)isoquinoline (2.92 g, 11.45 mmol) and 1.5 mL of water. The reaction vessel was evacuated and refilled with nitrogen (3 times), followed by the addition of $Pd(dppf)_2Cl_2{\cdot}CH_2Cl_2$ (623 mg, 0.76 mmol). The resulting mixture was stirred at 90 ℃ overnight and then cooled to room temperature. The mixture was diluted with EA (30 mL) and filtrated. The filtrate was sequentially washed by water, brine and dried over anhydrous Na_2SO_4. The organic layer was concentrated under vacuum and purified by silica gel column chromatography (MeOH/DCM, 1/100- 1/50) to afford compound **12a** as a white solid (1.97 g, 69% yield). ^{1}H NMR (400 MHz, CD_3OD) δ 9.25 (s, 1H), 8.45 (d, *J* = 5.8 Hz, 1H), 8.11 (d,

J = 8.5 Hz, 1H), 7.81 (d, *J* = 5.6 Hz, 2H), 7.74 (d, *J* = 2.7 Hz, 1H), 7.63 (d, *J* = 8.3 Hz, 1H), 7.40 (d, *J* = 7.4 Hz, 2H), 7.34 (t, *J* = 7.4 Hz, 2H), 7.26 (t, *J* = 7.1 Hz, 1H), 7.05 (d, *J* = 2.7 Hz, 1H), 4.51 (dd, *J* = 7.3, 4.7 Hz, 1H), 3.78 (ddd, *J* = 18.8, 11.1, 6.2 Hz, 2H). LRMS $[M+H]^+$: 376.1.

(*R*)-5-(2-Chloro-5-(2-hydroxy-1-phenylethylamino)pyridin-3-yl)indolin-2-one (12b). Compound **12b** was prepared in a similar manner as described for compound **12a.** Yield: 64%; ^{1}H NMR (400 MHz, CD_3OD) δ 7.63 (d, *J* = 2.9 Hz, 1H), 7.39 (d, *J* = 7.2 Hz, 2H), 7.34 (t, *J* = 7.5 Hz, 2H), 7.26 (t, *J* = 7.2 Hz, 1H), 7.20 (s, 1H), 7.14 (d, *J* = 8.0 Hz, 1H), 6.92 (t, *J* = 6.0 Hz, 2H), 4.47 (dd, *J* = 7.8, 4.6 Hz, 1H), 3.76 (ddd, *J* = 19.1, 11.2, 6.3 Hz, 2H), 3.55 (s, 2H). LRMS $[M+H]^+$: 380.1.

(*R*)-*N*-(4-(2-chloro-5-(2-hydroxy-1-phenylethylamino)pyridin-3-yl)phenyl)acetamide (12c). Compound **12c** was prepared in a similar manner as described for compound **12a.** Yield: 68%; LRMS $[M+H]^+$: 382.1.

(*R*)-2-(6-Chloro-5-(1H-indol-5-yl)pyridin-3-ylamino)-2-phenylethanol (12d). Compound **12d** was prepared in a similar manner as described for compound **12a.** Yield: 72%; LRMS $[M+H]^+$: 364.0.

(S)-2-(5-Bromo-6-chloropyridin-3-ylamino)-2-phenylethanol (13a). Compound **13a** was prepared in a similar manner as described for compound **10.** Yield: 51%; ^{1}H NMR (400 MHz, CD_3OD) δ 7.66 (d, *J* = 2.7 Hz, 1H), 7.40 – 7.32 (m, 4H), 7.26 (t, *J* = 6.8 Hz, 1H), 7.21 (d, *J* = 2.7 Hz, 1H), 4.42 (dd, *J* = 7.8, 4.6 Hz, 1H), 3.74 (ddd, *J* = 19.1, 11.3, 6.3 Hz, 2H). LRMS $[M+H]^+$: 328.9.

(*R*)-2-(5-Bromo-6-chloropyridin-3-ylamino)ethanol (13b). Compound **13b** was

prepared in a similar manner as described for compound **15.** Yield: 48%; LRMS $[M+H]^+$: 253.0.

(*R*)-3-(5-Bromo-6-chloropyridin-3-ylamino)propan-1-ol (13c). Compound **13c** was prepared in a similar manner as described for compound **15.** Yield: 45%; LRMS $[M+H]^+$: 267.0

(*S*)-2-(6-Chloro-5-(3-methyl-1H-indazol-5-yl)pyridin-3-ylamino)-2-phenylethanol (14a). Compound **14a** was prepared in a similar manner as described for compound **16a.** Yield: 53%; ^{1}H NMR (400 MHz, CD_3OD) δ 7.67 (d, *J* = 2.9 Hz, 1H), 7.55 – 7.51 (m, 1H), 7.46(d, *J* = 8.6 Hz, 1H), 7.43 – 7.37 (m, 2H), 7.36 – 7.31 (m, 3H), 7.30 – 7.22 (m, 1H), 6.97 (d, *J* = 2.9 Hz, 1H), 4.49 (dd, *J* = 7.8, 4.8 Hz, 1H), 3.82 (dd, *J* = 11.2, 4.8 Hz, 1H), 3.73 (dd, *J* = 11.2, 7.9 Hz, 1H), 2.56 (d, *J* = 12.6 Hz, 3H). LRMS $[M+H]^+$: 379.1

(*R*)-2-(6-Chloro-5-(3-methyl-1H-indazol-5-yl)pyridin-3-ylamino)ethanol (14b). Compound **14b** was prepared in a similar manner as described for compound **16a.** Yield: 42%; ^{1}H NMR (400 MHz, DMSO-d_6) δ 12.76 (s, 1H), 7.79 (d, *J* = 2.9 Hz, 1H), 7.74 (s, 1H), 7.52 (d, *J* = 8.5 Hz, 1H), 7.39 (dd, *J* = 8.6, 1.4 Hz, 1H), 7.06 (d, *J* = 2.9 Hz, 1H), 6.11 (t, *J* = 5.8 Hz, 1H), 4.76 (t, *J* = 5.3 Hz, 1H), 3.57 (q, *J* = 5.7 Hz, 2H), 3.17 (dd, *J* = 11.4, 5.7 Hz, 2H), 2.51 (s, 3H). LRMS $[M+H]^+$: 303.0.

(*R*)-2-(6-Chloro-5-(3-methyl-1H-indazol-5-yl)pyridin-3-ylamino)ethanol (14c). Compound **14c** was prepared in a similar manner as described for compound **16a.** Yield: 48%; ^{1}H NMR (400 MHz, DMSO-d_6) δ 12.75 (s, 1H), 7.75 (d, *J* = 2.7 Hz, 2H), 7.52 (d, *J* = 8.6 Hz, 1H), 7.39 (dd, *J* = 8.6, 1.4 Hz, 1H), 7.01 (d, *J* = 2.9 Hz, 1H), 6.10

(t, J = 5.4 Hz, 1H), 4.52 (t, J = 5.1 Hz, 1H), 3.51 (dd, J = 11.5, 6.1 Hz, 2H), 3.13 (dd, J = 12.7, 6.7 Hz, 2H), 2.51 (s, 3H), 1.71 (p, J = 6.5 Hz, 2H). LRMS $[M+H]^+$: 317.1

Kinase profiling

Kinase profiling

The kinase profiling of compounds was used by various methods: the kinase of Erk was tested by Fluorescence Resonance Energy Transfer (FRET)-based assay with Z′-LYTE™ Kinase Assay Kit (Invitrogen, Grand Island, NY), the kinases of CDK1, CDK4, CDK6 were detected by Fluorescence Resonance Energy Transfer (FRET)-based assay with LANCE Ultra Kinase Assay Kit (PerkinElmer, Waltham, Massachusetts), and other kinases used Elisa kinase assay as below.

ELISA kinase assay

The effects of indicated compound on the activities of various tyrosine kinases were determined using enzyme-linked immunosorbent assays (ELISAs) with purified recombinant proteins. Briefly, 20 μg/mL poly (Glu, Tyr) 4:1 (Sigma, St Louis, MO, USA) was pre-coated in 96-well plates as a substrate. A 50-μL aliquot of 10 μM ATP solution diluted in kinase reaction buffer (50 mM HEPES [pH 7.4], 50 mM $MgCl_2$, 0.5 mM $MnCl_2$, 0.2 mM Na_3VO_4, and 1 mM DTT) was added to each well; 1 μL of indicated compound diluted in 1% DMSO (v/v) (Sigma, St Louis, MO, USA) were then added to each reaction well. DMSO (1%, v/v) was used as the negative control. The kinase reaction was initiated by the addition of purified tyrosine kinase proteins diluted in 49μL of kinase reaction buffer. After incubation for 60 min at 37 ℃, the plate was washed three times with phosphate-buffered saline (PBS) containing 0.1%

Tween 20 (T-PBS). Anti-phosphotyrosine (PY99) antibody (100 μL; 1:500, diluted in 5 mg/mL BSA T-PBS) was then added. After a 30-min incubation at 37 °C, the plate was washed three times, and 100 μL horseradish peroxidase-conjugated goat anti-mouse IgG (1:1000, diluted in 5 mg/mL BSA T-PBS) was added. The plate was then incubated at 37 °C for 30 min and washed 3 times. A 100 μL aliquot of a solution containing 0.03% H_2O_2 and 2 mg/mL o-phenylenediamine in 0.1 M citrate buffer (pH 5.5) was added. The reaction was terminated by the addition of 50 μL of 2 M H_2SO_4 as the color changed, and the plate was analyzed using a multi-well spectrophotometer (SpectraMAX190, from Molecular Devices, Palo Alto, CA, USA) at 490 nm. The inhibition ratio (%) was calculated using the following equation: [1-(A490/A490 control)] ×100%. The IC_{50} values were calculated from the inhibition curves in two separate experiments.

Western blot analysis

NCI-H1581, KG1, SNU16, KATOIII, UMUC14, RT112, HCC827, PC-9, Ba/F3/CCDC6-RET and Ba/F3/TEL-KDR cells were treated with the indicated dose of **3m** for 2 h at 37 °C and then lysed in 1×SDS sample buffer. The cell lysates were subsequently resolved by 10% SDS-PAGE and transferred to nitrocellulose membranes. The membranes were probed with the appropriate primary antibodies [phospho-FGFR1, FGFR1, phospho-FGFR2, FGFR2, phospho-FGFR3, FGFR3, phospho-DDR2, DDR2, phospho-RET, RET, phospho-KDR, KDR, phospho-FRS2, FRS2, phosphor-ERK, ERK, PLCγ, phosphor–PLCγ, phospho-SRC, SRC, phospho-STAT3, STAT3, phospho-AKT, AKT, Tubulin, GAPDH (all from Cell

Signaling Technology, Beverly, MA, USA)] and then with horseradish peroxidase-conjugated anti-rabbit or anti- mouse IgG. The immune reactive proteins were detected using an enhanced chemilluminescense detection reagent (Thermo Fisher Scientific, Rockford, IL, USA)

Cell proliferation assay

Cells were seeded in 96-well cell culture plates. On the day when seeding, the cells were exposed to various concentrations of compounds and further cultured for 72 h at 37°C. Cell proliferation was then determined using Cell Counts Kit-8 (CCK8). The IC_{50} values were calculated by concentration-response curve fitting using the four-parameter method.

***In vivo* antitumor activity assay**

Female nude mice (4−6 weeks) were housed at five or six mice per cage in a specific pathogen free room with a 12 h light/dark schedule at 25 ± 1°C; the animals were fed an autoclaved chow diet and water ad libitum. All the animal experiments were performed according to the institutional ethical guidelines of animal care.

NCI-H1581 cells at a density of 5×10^6 were first implanted subcutaneously into the right flank of each mouse and then allowed to grow to 700-800 mm^3, which was defined as a well-developed tumor. The well-developed tumors were cut into 1.5mm^3 fragments and transplanted subcutaneously into the right flank of nude mice using a tracer. When the tumor volume reached 100-150 mm^3, the mice were randomly assigned into control vehicle and treatment groups (n = 6 in treated group, n=12 in vehicle group). The control groups were given vehicle alone, and the treatment groups

received **3m** at the indicated doses via oral administration once daily for 14 days. **16** was a positive Drug. The sizes of the tumors were measured twice per week using micro calipers. The tumor volume (TV) was calculated as follows: TV = (length × width^2)/2. The tumor volume shown was obtained on the indicated days as the median tumor volume ± SEM for indicated groups of mice. The relative tumor volume values, RTV, were measured on the final day of the study for the drug-treated mice compared with the vehicle-treated mice and were calculated as RTV = Vt/V_0, while V_0 is the tumor volume at day 0, Vt is the tumor volume measured each time point. The percentage of tumor volume inhibition values (TGI) was also measured. Significant differences between the treated versus the control groups ($P \leq 0.05$) were determined using Student's t test.

Pharmacokinetic profiles in SD rats and CD-1 mice

Compound **3m** (5% DMSO + 5% Tween-80 in 90% saline) was subjected to PK studies in SD rats and CD-1 mice. Compound **3m** was administered *via* the oral route at 20 mg/kg and administered *via* the intravenous route at 10 mg/kg in SD rats. Compound **3m** was administered *via* the oral route at 20 mg/kg and 5 mg/kg in CD-1 mice. After oral and intravenous administration, blood samples were collected. The blood samples were centrifuged to obtain the plasma fraction. The plasma samples were deproteinized with methanol containing an internal standard. After centrifugation, the supernatant was diluted with methanol and centrifuged again. The compound concentrations in the supernatant were measured by LC/MS/MS.

Acknowledgment

We gratefully acknowledge financial support from the National Natural Science Foundation of China Grants (21632008, 81620108027, and 81473243), NSFC-Shandong Joint Fund for Marine Science Research Centers (U1406402), Major Project of Chinese National Programs for Fundamental Research and Development (2015CB910304), and the Strategic Priority Research Program of the Chinese Academy of Sciences (XDA12050201).

Corresponding Author Information

Hong Liu Phone: 86-21-50807042. E-mail: hliu@simm.ac.cn.

Mingyue Zheng Phone: 86-021-50271399. E-mail: myzheng@simm.ac.cn.

Jing Ai Phone: 86-21-50806600 extension 2413. E-mail: jai@simm.ac.cn.

Supporting Information Available: SMILES strings of 57 candidate compounds, HPLC analysis data of all final compounds, illustration of the potential internal H-bond of compound **2m**, and the putative binding mode of **3m** with FGFR1 protein.

Abbreviations

NSCLC, non-small cell lung cancer; FGFR, fibroblast growth factor receptors; SAR, structure-activity relationship; EGFR, epidermal growth factor receptor;

TKIs, tyrosine kinase inhibitors; VEGFR, vascular endothelial growth factor receptor; PDGFR, platelet-derived growth factor receptor; CSF1R, colony-stimulating factor 1 receptor; TGI, tumor growth inhibition; PK, pharmacokinetic; AUC, area under the curve.

Reference

1. Jemal, A.; Siegel, R.; Ward, E.; Murray, T.; Xu, J.; Thun, M. J. Cancer statistics, 2007. *CA Cancer J. Clin*. **2007**, *57*, 43–66.
2. Zhou, Y.; Zhang, Y.; Zou, H.; Cai, N.; Chen, X.; Xu, L.; Kong, X.; Liu, P. The multi-targeted tyrosine kinase inhibitor vandetanib plays a bifunctional role in non-small cell lung cancer cells. *Sci Rep.* **2015**, *5*, 8629.
3. Lin, Y.; Wang, X.; Jin, H. EGFR-TKI resistance in NSCLC patients: mechanisms and strategies. *Am J. Cancer Res.* **2014**, *4*, 411-435.
4. Shea, M.; Costa, D. B. Rangachari, D. Management of advanced non-small cell lung cancers with known mutations or rearrangements: latest evidence and treatment approaches. *Ther. Adv. Respir. Dis.* **2016**, *10*, 113-129.
5. Beenken, A.; Mohammadi, M. The FGF family: biology, pathophysiology and therapy. *Nat. Rev. Drug Discovery* **2009**, *8*, 235-253.
6. Turner, N.; Grose, R. Fibroblast growth factor signalling: from development to cancer. *Nat. Rev. Cancer* **2010**, *10*, 116-129.
7. Weiss, J.; Sos, M. L.; Seidel, D.; Peifer, M.; Zander, T.; Heuckmann, J. M.; Ullrich, R. T.; Menon, R.; Maier, S.; Soltermann, A.; Moch, H.; Wagener, P.; Fischer, F.; Heynck, S.; Koker, M.; Schöttle, J.; Leenders, F.; Gabler, F.; Dabow, I.; Querings,

S.; Heukamp, L. C.; Balke-Want, H.; Ansén, S.; Rauh, D.; Baessmann, I.; Altmüller, J.; Wainer, Z.; Conron, M.; Wright, G.; Russell, P.; Solomon, B.; Brambilla, E.; Brambilla, C.; Lorimier, P.; Sollberg, S.; Brustugun, O. T.; Engel-Riedel, W.; Ludwig, C.; Petersen, I.; Sänger, J.; Clement, J.; Groen, H.; Timens, W.; Sietsma, H.; Thunnissen, E.; Smit, E.; Heideman, D.; Cappuzzo, F.; Ligorio, C.; Damiani, S.; Hallek, M.; Beroukhim, R.; Pao, W.; Klebl, B.; Baumann, M.; Buettner, R.; Ernestus, K.; Stoelben, E.; Wolf, J.; Nürnberg, P.; Perner, S.; Thomas, R. K. Frequent and focal FGFR1 amplification associates with therapeutically tractable FGFR1 dependency in squamous cell lung cancer. *Sci. Transl. Med.* **2010**, *2*, 62ra93.

8. Oxnard, G. R.; Binder, A.; Jänne, P. A. New targetable oncogenes in non-small-cell lung cancer. *J. Clin. Oncol.* **2013**, *31*, 1097-1104.
9. Zhao, G.; Li, W. Y.; Chen, D.; Henry, J. R.; Li, H. Y.; Chen, Z.; Zia-Ebrahimi, M.; Bloem, L.; Zhai, Y.; Huss, K.; Peng, S. B.; McCann, D. J. A novel, selective inhibitor of fibroblast growth factor receptors that shows a potent broad spectrum of antitumor activity in several tumor xenograft models. *Mol. Cancer Ther.* **2011,** 10, 2200-2210.
10. Inoue, K.; Torimura, T.; Nakamura, T.; Iwamoto, H.; Masuda, H.; Abe, M.; Hashimoto, O.; Koga, H.; Ueno, T.; Yano, H.; Sata, M. Vandetanib, an inhibitor of VEGF receptor-2 and EGF receptor, suppresses tumor development and improves prognosis of liver cancer in mice. *Clin. Cancer Res.* **2012,** 18, 3924-2933.
11. Matsui, J.; Yamamoto, Y.; Funahashi, Y.; Tsuruoka, A.; Watanabe, T.;

Wakabayashi, T.; Uenaka, T.; Asada, M. E7080, a novel inhibitor that targets multiple kinases, has potent antitumor activities against stem cell factor producing human small cell lung cancer H146, based on angiogenesis inhibition. *Int. J. Cancer* **2008,** 122, 664-671.

12. Roth, G. J.; Heckel, A.; Colbatzky, F.; Handschuh, S.; Kley, J.; Lehmann-Lintz, T.; Lotz, R.; Tontsch-Grunt, U.; Walter, R.; Hilberg, F. Design, synthesis, and evaluation of indolinones as triple angiokinase inhibitors and the discovery of a highly specific 6-methoxycarbonyl-substituted indolinone (BIBF 1120). *J. Med. Chem.* **2009,** 52, 4466-4480.
13. Gozgit, J. M.; Wong, M. J.; Wardwell, S.; Tyner, J. W.; Loriaux, M. M.; Mohemmad, Q. K.; Narasimhan, N. I.; Shakespeare, W. C.; Wang, F.; Druker, B. J.; Clackson, T.; Rivera, V. M. Potent activity of ponatinib (AP24534) in models of FLT3-driven acute myeloid leukemia and other hematologic malignancies. *Mol. Cancer Ther.* **2011,** 10, 1028-1035.
14. Sun, Y.; Niu, W.; Du, F.; Du, C.; Li, S.; Wang, J.; Li, L.; Wang, F.; Hao, Y.; Li, C.; Chi, Y. Safety, pharmacokinetics, and antitumor properties of anlotinib, an oral multi-target tyrosine kinase inhibitor, in patients with advanced refractory solid tumors. *J. Hematol. Oncol.* **2016,** 9, 105.
15. Morton, C. L.; Maris, J. M.; Keir, S. T.; Gorlick, R.; Kolb, E. A.; Billups, C. A.; Wu, J.; Smith, M. A.; Houghton, P. J. Combination testing of cediranib (AZD2171) against childhood cancer models by the pediatric preclinical testing program. *Pediatr. Blood Cancer* **2012,** 58, 566-571.

16. Bello, E.; Colella, G.; Scarlato, V.; Oliva, P.; Berndt, A.; Valbusa, G.; Serra, S. C.; D'Incalci, M.; Cavalletti, E.; Giavazzi, R.; Damia, G.; Camboni, G. E-3810 is a potent dual inhibitor of VEGFR and FGFR that exerts antitumor activity in multiple preclinical models. *Cancer Res.* **2011,** 71, 1396-1405.

17. Bhide, R. S.; Cai, Z. W.; Zhang, Y. Z.; Qian, L.; Wei, D.; Barbosa, S.; Lombardo, L. J.; Borzilleri, R. M.; Zheng, X.; Wu, L. I.; Barrish, J. C.; Kim, S. H.; Leavitt, K.; Mathur, A.; Leith, L.; Chao, S.; Wautlet, B.; Mortillo, S.; Jeyaseelan, R., Sr.; Kukral, D.; Hunt, J. T.; Kamath, A.; Fura, A.; Vyas, V.; Marathe, P.; D'Arienzo, C.; Derbin, G.; Fargnoli, J. Discovery and preclinical studies of (R)-1-(4-(4-fluoro-2-methyl-1H-indol-5-yloxy)-5-methylpyrrolo[2,1-f][1,2,4]triazin-6-yloxy)propan- 2-ol (BMS-540215), an in vivo active potent VEGFR-2 inhibitor. *J. Med. Chem.* **2006,** 49, 2143-2146.

18. Fei, F.; Lim, M.; Schmidhuber, S.; Moll, J.; Groffen, J.; Heisterkamp, N. Treatment of human pre-B acute lymphoblastic leukemia with the Aurora kinase inhibitor PHA-739358 (Danusertib). *Mol. Cancer* **2012,** 11, 42.

19. Cohen, R. B.; Langer, C. J.; Simon, G. R.; Eisenberg, P. D.; Hainsworth, J. D.; Madajewicz, S.; Cosgriff, T. M.; Pierce, K.; Xu, H.; Liau, K.; Healey, D. A phase I/randomized phase II, non-comparative, multicenter, open label trial of CP-547,632 in combination with paclitaxel and carboplatin or paclitaxel and carboplatin alone as first-line treatment for advanced non-small cell lung cancer (NSCLC). *Cancer Chemother. Pharmacol.* **2007,** 60, 81-89.

20. Moreno, L.; Marshall, L. V.; Pearson, A. D.; Morland, B.; Elliott, M.;

Campbell-Hewson, Q.; Makin, G.; Halford, S. E.; Acton, G.; Ross, P.; Kazmi-Stokes, S.; Lock, V.; Rodriguez, A.; Lyons, J. F.; Boddy, A. V.; Griffin, M. J.; Yule, M.; Hargrave, D. A phase I trial of AT9283 (a selective inhibitor of aurora kinases) in children and adolescents with solid tumors: a Cancer Research UK study. *Clin. Cancer Res.* **2015,** 21, 267-273.

21. Wesche, J.; Haglund, K.; Haugsten, E. M. Fibroblast growth factors and their receptors in cancer. *Biochem. J.* **2011**, *437*, 199-213.
22. Turner, N.; Pearson, A.; Sharpe, R.; Lambros, M.; Geyer, F.; Lopez-Garcia, M. A.; Natrajan, R.; Marchio, C.; Iorns, E.; Mackay, A.; Gillett, C.; Grigoriadis, A.; Tutt, A.; Reis-Filho, J. S.; Ashworth, A. FGFR1 amplification drives endocrine therapy resistance and is a therapeutic target in breast cancer. *Cancer Res.* **2010**, *70*, 2085-2094.
23. Dutt, A.; Salvesen, H. B.; Chent, T. H.; Ramos, A. H.; Onofrio, R. C.; Hatton, C.; Nicoletti, R.; Winckler, W.; Grewal, R.; Hanna, M.; Wyhs, N.; Ziaugra, L.; Richter, D. J.; Trovik, J.; Engelsen, I. B.; Stefansson, I. M.; Fennell, T.; Cibulskis, K.; Zody, M. C.; Akslen, L. A.; Gabriel, S.; Wong, K. K.; Sellers, W. R.; Meyerson, M.; Greulich, H. Drug-sensitive FGFR2 mutations in endometrial carcinoma. *Proc. Natl. Acad. Sci. U S A.* **2008**, *105*, 8713-8717.
24. Shoichet, B. K. Virtual screening of chemical libraries. *Nature* **2004**, *432*, 862-865.
25. Zhang, L.; Zheng, M. Y.; Zhao, F.; Zhai, Y.; Liu, H. Rapid generation of privileged substructure-based compound libraries with structural diversity and drug-likeness.

ACS Comb. Sci. **2014**, *16*, 184-191.

26. Drewry, D. H.; Macarron, R. Enhancements of screening collections to address areas of unmet medical need: an industry perspective. *Curr. Opin. Chem. Biol.* **2010**, *14*, 289-298.
27. Bleicher, K. H.; Bohm, H. J.; Muller, K.; Alanine, A. I. Hit and lead generation: beyond high-throughput screening. *Nat. Rev. Drug Discovery* **2003**, *2*, 369-378.
28. Spandl, R. J.; Bender, A.; Spring, D. R. Diversity-oriented synthesis; a spectrum of approaches and results. *Org. Biomol. Chem.* **2008**, *6*, 1149-1158.
29. Golebiowski, A.; Klopfenstein, S. R.; Portlock, D. E. Lead compounds discovered from libraries. *Curr. Opin. Chem. Biol.* **2001**, *5*, 273-284.
30. Geysen, H. M.; Schoenen, F.; Wagner, D.; Wagner, R. Combinatorial compound libraries for drug discovery: An ongoing challenge. *Nat. Rev. Drug Discovery* **2003**, *2*, 222-230.
31. Orry, A. J. W.; Abagyan, R. A.; Cavasotto, C. N. Structure-based development of target-specific compound libraries. *Drug Discovery Today* **2006**, *11*, 261-266.
32. Welsch, M. E.; Snyder, S. A.; Stockwell, B. R. Privileged scaffolds for library design and drug discovery. *Curr. Opin. Chem. Biol.* **2010**, *14*, 347-361.
33. Lopez-Vallejo, F.; Giulianotti, M. A.; Houghten, R. A.; Medina-Franco, J. L. Expanding the medicinally relevant chemical space with compound libraries. *Drug Discovery Today* **2012**, *17*, 718-726.
34. Guagnano, V.; Furet, P.; Spanka, C.; Bordas, V.; Le Douget, M.; Stamm, C.; Brueggen, J.; Jensen, M. R.; Schnell, C.; Schmid, H.; Wartmann, M.; Berghausen,

J.; Drueckes, P.; Zimmerlin, A.; Bussiere, D.; Murray, J.; Graus Porta, D. Discovery of 3-(2,6-dichloro-3,5-dimethoxy-phenyl)-1-{6-[4-(4-ethyl-piperazin-1-yl)-phenylamin o]-pyrimidin-4-yl}-1-methyl-urea (NVP-BGJ398), a potent and selective inhibitor of the fibroblast growth factor receptor family of receptor tyrosine kinase. *J. Med. Chem.* **2011**, *54*, 7066-7083.

35. Friesner, R. A.; Murphy, R. B.; Repasky, M. P.; Frye, L. L.; Greenwood, J. R.; Halgren, T. A.; Sanschagrin, P. C.; Mainz, D. T. Extra precision glide: docking and scoring incorporating a model of hydrophobic enclosure for protein-ligand complexes. *J. Med. Chem.* **2006**, *49*, 6177-6196.
36. Gavine, P.; Mooney, L,; Kilgour E.; Thomas A.; Al-Kadhimi K.; Beck S.; Rooney C.; Coleman T.; Baker D.; Mellor M.; Brooks A.; Klinowska T.; AZD4547: an ora lly bioavailable, potent, and selective inhibitor of the fibroblast growth factor rece ptor tyrosine kinase family. *Cancer Res.* **2012**, *72*, 2045-2056.
37. Cheng, Z.; Han, X.; Jiang, M.; Wang, J.; Wang, M.; Yang, S.; Zhou, C. New substituted pyridine compounds used for treating cancers e.g. glioma, colorectal and pancreatic cancers and cancers of larynx, lymphatic system, liver, and skin. WO2014/090692, June 19, 2014.
38. Wang, J.; Sanchez-Rosello, M.; Acena, J. L.; del Pozo, C.; Sorochinsky, A. E.; Fustero, S.; Soloshonok, V. A.; Liu, H. Fluorine in pharmaceutical industry: fluorine-containing drugs introduced to the market in the last decade (2001-2011). *Chem. Rev.* **2014**, *114*, 2432-2506.

39. Zhou, Y.; Wang, J.; Gu, Z.; Wang, S.; Zhu, W.; Acena, J. L.; Soloshonok, V. A.; Izawa, K.; Liu, H. Next generation of fluorine-containing pharmaceuticals, compounds currently in phase II-III clinical trials of major pharmaceutical companies: new structural trends and therapeutic areas. *Chem. Rev.* **2016**, *116*, 422-518.

40. Guagnano, V.; Kauffmann, A.; Wohrle, S.; Stamm, C.; Ito, M.; Barys, L.; Pornon, A.; Yao, Y.; Li, F.; Zhang, Y.; Chen, Z.; Wilson, C. J.; Bordas, V.; Le Douget, M.; Gaither, L. A.; Borawski, J.; Monahan, J. E.; Venkatesan, K.; Brummendorf, T.; Thomas, D. M.; Garcia-Echeverria, C.; Hofmann, F.; Sellers, W. R.; Graus-Porta, D. FGFR genetic alterations predict for sensitivity to NVP-BGJ398, a selective pan-FGFR inhibitor. *Cancer Discovery* **2012**, *2*, 1118-1133.

Table of Contents Graphic

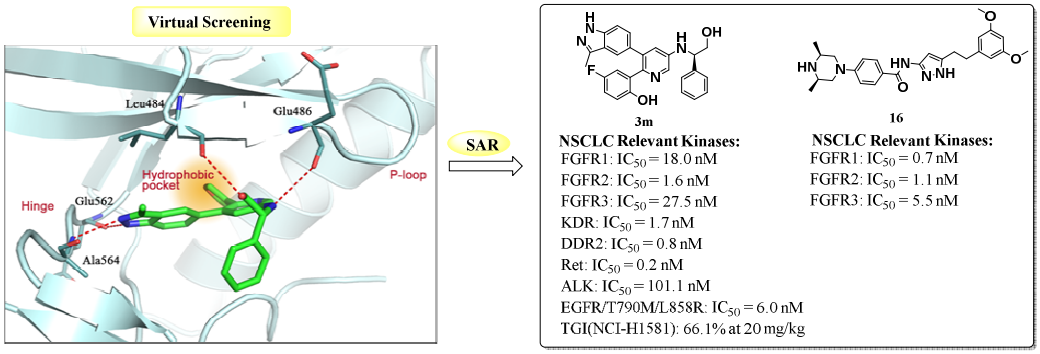

Table of Contents Graphic